Acta Mech 227, 2377–2401 (2016)
DOI 10.1007/s00707-016-1637-y

ORIGINAL PAPER

Dao Van Dung · Nguyen Thi Nga

Buckling and postbuckling nonlinear analysis of imperfect FGM plates reinforced by FGM stiffeners with temperature-dependent properties based on TSDT

Received: 13 January 2016 / Revised: 30 March 2016 / Published online: 3 May 2016

Abstract Using Reddy's third-order shear deformation plate theory (TSDT) with von Kármán geometrical nonlinearity, this work presents an analytical solution on the buckling and postbuckling behaviors of eccentrically stiffened functionally graded material (ES-FGM) plates on elastic foundations subjected to in-plane compressive loads or thermal loads or thermo-mechanical loads. Plates are reinforced by closely spaced FGM stiffeners. The material properties of the plate and stiffeners are assumed to be temperature-dependent. Theoretical formulations based on the smeared stiffeners technique and TSDT are derived. The expressions of thermal parameters are found in the analytical form. Applying Galerkin method, the expressions to determine the critical buckling load and analyze the postbuckling mechanical and thermal load–deflection curves are obtained. Two iterative algorithms are presented for the case of temperature-dependent plate material properties. The effects of thermal element, FGM stiffeners, geometrical and material parameters, initial imperfection, and foundation are considered and discussed. By comparing the present results with those in references, the accuracy of the present study is affirmed.

1 Introduction

Functionally graded materials (FGMs) composed of ceramic and metal constituents have received much interest in recent years. Due to essential characteristics such as high stiffness and excellent temperature resistance capacity, functionally graded materials have found wide applications in many industries, especially in temperature shielding structures and nuclear plants, where significant changes in material properties are unavoidable. As a result, many researches focused on the buckling and postbuckling analyses of plates made of FGM.

Ferreira et al. [1] employed the higher-order shear deformation theory to analyze the buckling of isotropic and laminated plates by radial basis functions. Shariat and Eslami [2] presented the buckling analysis of rectangular thick functionally graded plates under mechanical and thermal loads based on the TSDT. Khabbaz et al. [3] studied the nonlinear analysis of FGM plates under pressure loads using the first-order shear deformation theory (FSDT) and TSDT. Duc and Tung [4] investigated the buckling and postbuckling behaviors of un-stiffened functionally graded plates resting on elastic foundations and subjected to thermo-mechanical loads, in which the material properties are assumed to be temperature-independent. Javaheri and Eslami [5,6] investigated the stability of FGM plates subjected to mechanical and thermal loads based on the classical plate theory (CPT) with temperature-independent material properties (T-ID). The same authors [7] considered the thermal buckling of FGM plates based on the higher-order theory. The results of three- dimensional thermo-mechanical buckling analysis for a composite FGM plate by using the finite element method were investigated by Na and Kim [8]. Lanhe [9] presented an analytical solution for the thermal buckling of an FGM rectangular

D. V. Dung · N. T. Nga (✉)
Vietnam National University, Hanoi, Vietnam
E-mail: nguyennga282@gmail.com
Tel.: +84 932284586

simply supported plate subjected to a uniform temperature rise and gradient through the thickness of the plate. The buckling of heated FGM annular plates on an elastic foundation was studied analytically by Kiani and Eslami [10].

For un-stiffened shells, many researches are focused on the buckling and postbuckling analysis of shells. Hui and Du [11] studied initial postbuckling behaviors of imperfect antisymmetric crossply cylindrical shells under torsion. Using singular perturbation technique, Zhang and Han [12] investigated the buckling and postbuckling of imperfect cylindrical shells subjected to torsion based on the Kármán–Donnell-type nonlinear differential equations. Jiang et al. [13] presented mechanical, electrical and thermal properties of aligned carbon nanotube/polyimide. Based on the higher-order shear deformation shell theory, Bagherizadeh et al. [14] investigated the mechanical buckling of FGM un-stiffened cylindrical shells surrounded by a Pasternak elastic foundation. Many investigations on the stability and vibration analysis of FGM un-stiffened cylindrical shells surrounded by elastic foundations also have been published by Sofiyev et al. [15–17]. Sofiyev [18–20] studied the nonlinear buckling of an FGM truncated conical shell with and without elastic foundations under an axial load using classical shell theory (CST).

With temperature-dependent material properties (T-D), there are some significant results. Shen [21,22] presented the thermal postbuckling behavior of an FGM plate and cylindrical shell. Shen [23] also investigated a nonlinear bending analysis of a simply supported FGM plate resting on an elastic foundation based on a higher-order shear deformation plate theory. Lal et al. [24] examined the second-order statistics of the postbuckling response of an FGM plate subjected to mechanical and thermal loading. Akbari et al. [25] performed a thermal buckling analysis of temperature-dependent FGM conical shells based on an iterative generalized differential quadrature method. Mirzavand and Eslami [26] presented a closed-form solution for thermal buckling of piezoelectric FGM rectangular plates based on TSDT.

Nowadays, the stiffened plate and shell structures are widely used in modern industry fields, such as ships, bridges, tank roofs and vehicles. Because the economical design of loaded structure can be obtained by using stiffeners instead of increasing the thickness of the structure, many researches have been published regarding structures reinforced by a system of stiffeners made of homogeneous material or functionally graded material. The analysis of the linear buckling of stiffened plates by the orthotropic plate method may be found in Timoshenko and Gere [27]. The elastic buckling and postbuckling behaviors of eccentrically stiffened plates were evaluated analytically by Steen [28], using the simplified direct energy approach together with Marguerre's plate theory. The influence of stiffener location on the stability of stiffened plates under compression and in-plane bending was studied by Bedair [29]. Bich et al. [30] investigated the nonlinear static buckling behavior of eccentrically stiffened imperfect FGM plates and shallow shells and the nonlinear dynamic response of eccentrically stiffened imperfect FGM panels on the basis of the classical plate and shell theory. Stiffeners in these researches [27–30] were assumed to be homogenous.

Following the direction of FGM stiffeners, Najafizadeh et al. [31] with the stability equation given in terms of displacement investigated the mechanical buckling behavior of FGM stiffened cylindrical shells reinforced by rings and stringers using CST. Dung and Nam [32] presented a nonlinear dynamic analysis of eccentrically stiffened functionally graded thin circular cylindrical shells surrounded by an elastic medium based on CST. Dung et al. [33] investigated the stability of functionally graded truncated conical shells surrounded by an elastic medium. Dung and Hoa [34] presented the nonlinear buckling and postbuckling of functionally graded stiffened thin circular cylindrical shells under torsional load surrounded by elastic foundations in thermal environments according to CST.

In this paper, the nonlinear analyses on the buckling and postbuckling behavior of imperfect FGM plates reinforced by FGM stiffeners with temperature-dependent material properties based on Reddy's third-order shear deformation theory [35–37] are investigated. The explicit expressions to determine the critical buckling load and analyze the postbuckling mechanical and thermal load–deflection curves are obtained. Two iterative algorithms are presented for the case of temperature-dependent plate material properties. The effects of thermal element, FGM stiffeners, geometrical and material parameters, initial imperfections and foundations are considered and discussed.

2 Eccentrically stiffened FGM plates (ES-FGM plates)

Consider a functionally graded rectangular plate of length a, width b and uniform thickness h. Assume that the plate is reinforced by closely spaced the longitudinal and transversal stiffeners. The thickness and width of the longitudinal stiffeners are h_1, b_1. The thickness and width of the transversal stiffeners are h_2, b_2. The distance

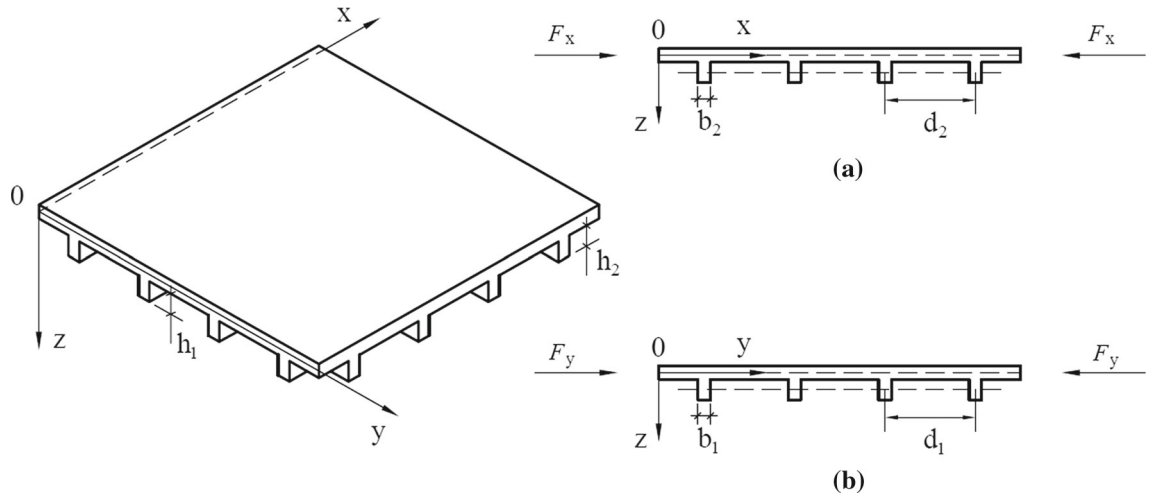

Fig. 1 Configuration of an eccentrically stiffened FGM plate

between two longitudinal stiffeners and two transversal stiffeners is d_1, d_2, respectively. The coordinate system (x, y, z) is chosen as shown in Fig. 1. The plane Oxy coincides with the un-deformed middle surface of the plate, and the axis $0z$ is in the thickness direction $(-h/2 \le z \le h/2)$.

The functionally graded materials of plates and stiffeners are assumed to be varied continuously in the thickness direction and made from a mixture of ceramic and metal.

Assume that the modulus of elasticity, coefficient of thermal expansion, thermal conductivity coefficient of plates and stiffeners depend on temperature with the rule of mixtures, [36,38];

For the plate:

$$\begin{aligned}
E_{\mathrm{p}}(z,T) &= E_{\mathrm{m}}(T) + E_{\mathrm{cm}}(T)\left(\frac{2z+h}{2h}\right)^{k}, \quad E_{\mathrm{cm}}(T) = E_{\mathrm{c}}(T) - E_{\mathrm{m}}(T) = -E_{\mathrm{mc}}(T),\\
\alpha_{\mathrm{p}}(z,T) &= \alpha_{\mathrm{m}}(T) + \alpha_{\mathrm{cm}}(T)\left(\frac{2z+h}{2h}\right)^{k}, \quad \alpha_{\mathrm{cm}}(T) = \alpha_{\mathrm{c}}(T) - \alpha_{\mathrm{m}}(T) = -\alpha_{\mathrm{mc}}(T),\\
\kappa_{\mathrm{p}}(z,T) &= \kappa_{\mathrm{m}}(T) + \kappa_{\mathrm{cm}}(T)\left(\frac{2z+h}{2h}\right)^{k}, \quad \kappa_{\mathrm{cm}}(T) = \kappa_{\mathrm{c}}(T) - \kappa_{\mathrm{m}}(T) = -\kappa_{\mathrm{mc}}(T);
\end{aligned} \tag{1}$$

for longitudinal stiffeners:

$$\begin{aligned}
E_{\mathrm{s}x}(z,T) &= E_{\mathrm{c}}(T) + E_{\mathrm{mc}}(T)\left(\frac{2z-h}{2h_1}\right)^{k_2}, \quad \frac{h}{2} \le z \le \frac{h}{2} + h_1,\\
\alpha_{\mathrm{s}x}(z,T) &= \alpha_{\mathrm{c}}(T) + \alpha_{\mathrm{mc}}(T)\left(\frac{2z-h}{2h_1}\right)^{k_2},\\
\kappa_{\mathrm{s}x}(z,T) &= \kappa_{\mathrm{c}}(T) + \kappa_{\mathrm{mc}}(T)\left(\frac{2z-h}{2h_1}\right)^{k_2};
\end{aligned} \tag{2}$$

for transversal stiffeners:

$$\begin{aligned}
E_{\mathrm{s}y}(z,T) &= E_{\mathrm{c}}(T) + E_{\mathrm{mc}}(T)\left(\frac{2z-h}{2h_2}\right)^{k_3}, \quad \frac{h}{2} \le z \le \frac{h}{2} + h_2,\\
\alpha_{\mathrm{s}y}(z,T) &= \alpha_{\mathrm{c}}(T) + \alpha_{\mathrm{mc}}(T)\left(\frac{2z-h}{2h_2}\right)^{k_3},\\
\kappa_{\mathrm{s}y}(z,T) &= \kappa_{\mathrm{c}}(T) + \kappa_{\mathrm{mc}}(T)\left(\frac{2z-h}{2h_2}\right)^{k_3};
\end{aligned} \tag{3}$$

where $k \geq 0, k_2 \geq 0, k_3 \geq 0$ are the volume fraction indices; the subscripts "m" and "c" refer to the metal and ceramic constituents, respectively; $E_{\mathrm{p}}(z), \alpha_{\mathrm{p}}(z), \kappa_{\mathrm{p}}(z)$ are Young's modulus, thermal expansion coefficient, and thermal conductivity coefficient of the plate; $E_{\mathrm{s}x}(z), \alpha_{\mathrm{s}x}(z), \kappa_{\mathrm{s}x}(z)$ and $E_{\mathrm{s}y}(z), \alpha_{\mathrm{s}y}(z), \kappa_{\mathrm{s}y}(z)$ are Young's modulus, thermal expansion coefficient, and thermal conductivity coefficient of x-direction and y-direction stiffeners, respectively.

Poisson's ratio is assumed to be a constant.

Assume that the plate is resting on an elastic foundation with the plate–foundation interaction determined by the Pasternak model as

$$q_f = K_1 w - K_2 \Delta w \tag{4}$$

where K_1 (N/m^3) is the Winkler foundation modulus, and K_2 (N/m) is the shear layer stiffness of the Pasternak model.

3 Basic relations and governing equations

Denote u, v, w the displacement components of the mid-plane of the plate in x, y, z direction, respectively, and ϕ_x, ϕ_y are the rotations of a transverse normal about the y- and x-axis, respectively.

According to Reddy's third-order shear deformation plate theory (TSDT) taking into account the von Kármán geometrical nonlinearity and an initial imperfection, the strain components across the plate thickness at a distance z from the mid-plane are of the form [35–37]

$$\begin{pmatrix} \varepsilon_x \\ \varepsilon_y \\ \gamma_{xy} \end{pmatrix} = \begin{pmatrix} \varepsilon_x^0 \\ \varepsilon_y^0 \\ \gamma_{xy}^0 \end{pmatrix} + z \begin{pmatrix} \kappa_x^1 \\ \kappa_y^1 \\ \kappa_{xy}^1 \end{pmatrix} + z^3 \begin{pmatrix} \kappa_x^{(3)} \\ \kappa_y^{(3)} \\ \kappa_{xy}^{(3)} \end{pmatrix}, \quad \begin{pmatrix} \gamma_{xz} \\ \gamma_{yz} \end{pmatrix} = \begin{pmatrix} \gamma_{xz}^0 \\ \gamma_{yz}^0 \end{pmatrix} + z^2 \begin{pmatrix} \kappa_{xz}^{(2)} \\ \kappa_{yz}^{(2)} \end{pmatrix} \tag{5}$$

where

$$\begin{pmatrix} \varepsilon_x^0 \\ \varepsilon_y^0 \\ \gamma_{xy}^0 \end{pmatrix} = \begin{pmatrix} u_{,x} + \frac{1}{2} w_{,x}^2 + w_{,x} w_{,x}^* \\ v_{,y} + \frac{1}{2} w_{,y}^2 + w_{,y} w_{,y}^* \\ u_{,y} + v_{,x} + w_{,x} w_{,y} + w_{,x} w_{,y}^* + w_{,y} w_{,x}^* \end{pmatrix}, \quad \begin{pmatrix} \gamma_{xz}^0 \\ \gamma_{yz}^0 \end{pmatrix} = \begin{pmatrix} \phi_x + w_{,x} \\ \phi_y + w_{,y} \end{pmatrix}, \quad \lambda = \frac{4}{3h^2}, \tag{6.1}$$

$$\begin{pmatrix} \kappa_x^1 \\ \kappa_y^1 \\ \kappa_{xy}^1 \end{pmatrix} = \begin{pmatrix} \phi_{x,x} \\ \phi_{y,y} \\ \phi_{x,y} + \phi_{y,x} \end{pmatrix}, \quad \begin{pmatrix} \kappa_x^{(3)} \\ \kappa_y^{(3)} \\ \kappa_{xy}^{(3)} \end{pmatrix} = -\lambda \begin{pmatrix} \phi_{x,x} + w_{,xx} \\ \phi_{y,y} + w_{,yy} \\ \phi_{x,y} + \phi_{y,x} + 2w_{,xy} \end{pmatrix}, \quad \begin{pmatrix} \kappa_{xz}^{(2)} \\ \kappa_{yz}^{(2)} \end{pmatrix} = -3\lambda \begin{pmatrix} \phi_x + w_{,x} \\ \phi_y + w_{,y} \end{pmatrix}, \tag{6.2}$$

in which $\varepsilon_x, \varepsilon_y$ are normal strains; γ_{xy} is the in-plane shear strain; γ_{xz}, γ_{yz} are the transverse shear deformations, and $w^* = w^*(x, y)$ is a known function representing the initial imperfection of the plate.

From Eq. (6.1), the geometric compatibility equation of the imperfect plate is represented in the form [37–39]

$$\varepsilon_{x,yy}^0 + \varepsilon_{y,xx}^0 - \gamma_{xy,xy}^0 = w_{,xy}^2 - w_{,xx} w_{,yy} - w_{,xx} w_{,yy}^* + 2w_{,xy} w_{,xy}^* - w_{,xx}^* w_{,yy}. \tag{7}$$

The stress–strain relations taking into account the temperature dependence of the plate material properties are defined by Hooke's law as [9,38,40]

$$\begin{aligned} \sigma_x^{\mathrm{p}} &= \frac{E_{\mathrm{p}}(z,T)}{1-\nu^2} \left[(\varepsilon_x + \nu \varepsilon_y) - (1+\nu) \alpha_{\mathrm{p}}(z,T) \Delta T \right], \\ \sigma_y^{\mathrm{p}} &= \frac{E_{\mathrm{p}}(z,T)}{1-\nu^2} \left[(\varepsilon_y + \nu \varepsilon_x) - (1+\nu) \alpha_{\mathrm{p}}(z,T) \Delta T \right], \\ \sigma_{xy}^{\mathrm{p}} &= \frac{E_{\mathrm{p}}(z,T)}{2(1+\nu)} \gamma_{xy}, \sigma_{xz}^{\mathrm{p}} = \frac{E_{\mathrm{p}}(z,T)}{2(1+\nu)} \gamma_{xz}, \quad \sigma_{yz}^{\mathrm{p}} = \frac{E_{\mathrm{p}}(z,T)}{2(1+\nu)} \gamma_{yz}, \end{aligned} \tag{8.1}$$

and for stiffeners taking into account the temperature [34,40]

$$\begin{aligned}\sigma_x^{\mathrm{s}} &= E_{\mathrm{s}x}(z,T)\,\varepsilon_x - E_{\mathrm{s}x}(z,T)\,\alpha_{\mathrm{s}x}(z,T)\,\Delta T,\\ \sigma_y^{\mathrm{s}} &= E_{\mathrm{s}y}(z,T)\,\varepsilon_y - E_{\mathrm{s}y}(z,T)\,\alpha_{\mathrm{s}y}(z,T)\,\Delta T,\\ \sigma_{xz}^{\mathrm{s}} &= G_{\mathrm{s}x}(z,T)\,\gamma_{xz},\ \sigma_{yz}^{\mathrm{s}} = G_{\mathrm{s}y}(z,T)\,\gamma_{yz}\end{aligned} \tag{8.2}$$

where $\Delta T = T - T_0$ denotes the change in the environment temperature from the initial free stress state; the superscripts "p" and "s" denote plate and stiffener, respectively; $G_{\mathrm{s}x}$, $G_{\mathrm{s}y}$ are shear moduli of x-direction and y-direction stiffeners, respectively.

The in-plane normal force intensities N_i, the bending moment intensities M_i and higher-order bending moment intensities P_i, transverse shearing force intensities Q_i and the higher-order shear force intensities R_i of functionally graded plates reinforced by FGM stiffeners are defined as

$$\begin{aligned}N_i &= \int_{-h/2}^{h/2}\sigma_i^{\mathrm{p}}\mathrm{d}z + N_i^{\mathrm{s}},\quad M_i = \int_{-h/2}^{h/2} z\sigma_i^{\mathrm{p}}\mathrm{d}z + M_i^{\mathrm{s}},\quad P_i = \int_{-h/2}^{h/2} z^3\sigma_i^{sh}\mathrm{d}z + P_i^{\mathrm{s}},\\ Q_i &= \int_{-h/2}^{h/2}\sigma_{iz}^{\mathrm{p}}\mathrm{d}z + Q_i^{\mathrm{s}},\quad R_i = \int_{-h/2}^{h/2} z^2\sigma_{iz}^{\mathrm{p}}\mathrm{d}z + R_i^{\mathrm{s}},\quad i = x, y,\\ N_{xy} &= \int_{-h/2}^{h/2}\sigma_{xy}^{\mathrm{p}}\mathrm{d}z,\quad M_{xy} = \int_{-h/2}^{h/2} z\sigma_{xy}^{\mathrm{p}}\mathrm{d}z,\quad P_{xy} = \int_{-h/2}^{h/2} z^3\sigma_{xy}^{\mathrm{p}}\mathrm{d}z\end{aligned} \tag{9}$$

where N_i^{s}, M_i^{s}, P_i^{s}, Q_i^{s}, R_i^{s} with $i = x, y$ are respective quantities for stiffeners.

Substituting Eqs. (5–6.1) and (8) in Eq. (9) and using the Lekhnitskii smeared stiffener technique, we obtain expressions like as [31,34,39]

$$\begin{aligned}N_x &= a_{11}\varepsilon_x^0 + a_{12}\varepsilon_y^0 + a_{13}\phi_{x,x} + a_{14}\phi_{y,y} + a_{15}w_{,xx} + a_{16}w_{,yy} + a_{17}\phi_1^{\mathrm{p}} + a_{18}\phi_1^{\mathrm{s}x},\\ N_y &= a_{21}\varepsilon_x^0 + a_{22}\varepsilon_y^0 + a_{23}\phi_{x,x} + a_{24}\phi_{y,y} + a_{25}w_{,xx} + a_{26}w_{,yy} + a_{27}\phi_1^{\mathrm{p}} + a_{28}\phi_1^{\mathrm{s}y},\\ N_{xy} &= a_{31}\gamma_{xy}^0 + a_{32}\phi_{x,y} + a_{33}\phi_{y,x} + a_{34}w_{,xy},\end{aligned} \tag{10}$$

$$\begin{aligned}M_x &= b_{11}\varepsilon_x^0 + b_{12}\varepsilon_y^0 + b_{13}\phi_{x,x} + b_{14}\phi_{y,y} + b_{15}w_{,xx} + b_{16}w_{,yy} + b_{17}\phi_2^{\mathrm{p}} + b_{18}\phi_2^{\mathrm{s}x},\\ M_y &= b_{21}\varepsilon_x^0 + b_{22}\varepsilon_y^0 + b_{23}\phi_{x,x} + b_{24}\phi_{y,y} + b_{25}w_{,xx} + b_{26}w_{,yy} + b_{27}\phi_2^{\mathrm{p}} + b_{28}\phi_2^{\mathrm{s}y},\\ M_{xy} &= b_{31}\gamma_{xy}^0 + b_{32}\phi_{x,y} + b_{33}\phi_{y,x} + b_{34}w_{,xy},\end{aligned} \tag{11}$$

$$\begin{aligned}P_x &= c_{11}\varepsilon_x^0 + c_{12}\varepsilon_y^0 + c_{13}\phi_{x,x} + c_{14}\phi_{y,y} + c_{15}w_{,xx} + c_{16}w_{,yy} + c_{17}\phi_4^{\mathrm{p}} + c_{18}\phi_4^{\mathrm{s}x},\\ P_y &= c_{21}\varepsilon_x^0 + c_{22}\varepsilon_y^0 + c_{23}\phi_{x,x} + c_{24}\phi_{y,y} + c_{25}w_{,xx} + c_{26}w_{,yy} + c_{27}\phi_4^{\mathrm{p}} + c_{28}\phi_4^{\mathrm{s}y},\\ P_{xy} &= c_{31}\gamma_{xy}^0 + c_{32}\phi_{x,y} + c_{33}\phi_{y,x} + c_{34}w_{,xy},\end{aligned} \tag{12}$$

$$\begin{aligned}Q_x &= d_{11}\phi_x + d_{12}w_{,x},\\ Q_y &= d_{21}\phi_y + d_{22}w_{,y},\end{aligned} \tag{13.1}$$

$$\begin{aligned}R_x &= e_{11}\phi_x + e_{12}w_{,x},\\ R_y &= e_{21}\phi_y + e_{22}w_{,y},\end{aligned} \tag{13.2}$$

where $\phi_1^{\mathrm{p}}, \phi_2^{\mathrm{p}}, \phi_4^{\mathrm{p}}, \phi_1^{\mathrm{s}x}, \phi_2^{\mathrm{s}x}, \phi_4^{\mathrm{s}x}, \phi_1^{\mathrm{s}y}, \phi_2^{\mathrm{s}y}, \phi_4^{\mathrm{s}y}$ are given by

$$\begin{aligned}\phi_j^{\mathrm{p}} &= \int_{-h/2}^{h/2} z^{j-1}E_{\mathrm{p}}(z,T)\,\alpha_{\mathrm{p}}(z,T)\,\Delta T\mathrm{d}z,\quad j = 1,2,4,\\ \phi_j^{\mathrm{s}x} &= \int_{h/2}^{h_1+h/2} z^{j-1}E_{\mathrm{s}x}(z,T)\,\alpha_{\mathrm{s}x}(z,T)\,\Delta T\mathrm{d}z,\quad \phi_j^{\mathrm{s}y} = \int_{h/2}^{h_2+h/2} z^{j-1}E_{\mathrm{s}y}(z,T)\,\alpha_{\mathrm{s}y}(z,T)\,\Delta T\mathrm{d}z,\quad j = 1,2,4,\end{aligned} \tag{14}$$

and the coefficients $a_{ij}, b_{ij}, c_{ij}, d_{ij}$ are defined in "Appendix I."

The relations (10–13.1) are the most significant contribution found in this work in which the thermal elements in plates and stiffeners are considered.

The strain–force resultant relations reversely are obtained from Eq. (10),

$$\begin{aligned}
\varepsilon_x^0 &= a_{11}^* N_x + a_{12}^* N_y + a_{13}^* \phi_{x,x} + a_{14}^* \phi_{y,y} + a_{15}^* w_{,xx} + a_{16}^* w_{,yy} + a_{17}^* \phi_1^{\mathrm{p}} + a_{18}^* \phi_1^{sx} + a_{19}^* \phi_1^{sy},\\
\varepsilon_y^0 &= a_{21}^* N_x + a_{22}^* N_y + a_{23}^* \phi_{x,x} + a_{24}^* \phi_{y,y} + a_{25}^* w_{,xx} + a_{26}^* w_{,yy} + a_{27}^* \phi_1^{\mathrm{p}} + a_{28}^* \phi_1^{sx} + a_{29}^* \phi_1^{sy},\\
\gamma_{xy}^0 &= a_{31}^* N_{xy} + a_{32}^* \phi_{x,y} + a_{33}^* \phi_{y,x} + a_{34}^* w_{,xy}
\end{aligned} \tag{15}$$

where

$$\begin{aligned}
&a_{11}^* = \frac{a_{22}}{a_{66}}, \quad a_{12}^* = -\frac{a_{12}}{a_{66}}, \quad a_{13}^* = \frac{a_{12}a_{23} - a_{22}a_{13}}{a_{66}}, \quad a_{14}^* = \frac{a_{12}a_{24} - a_{22}a_{14}}{a_{66}}, \quad a_{15}^* = \frac{a_{12}a_{25} - a_{22}a_{15}}{a_{66}},\\
&a_{16}^* = \frac{a_{12}a_{26} - a_{22}a_{16}}{a_{66}}, \quad a_{17}^* = \frac{a_{12}a_{27} - a_{22}a_{17}}{a_{66}}, \quad a_{18}^* = -\frac{a_{22}a_{18}}{a_{66}}, \quad a_{19}^* = \frac{a_{12}a_{28}}{a_{66}},\\
&a_{21}^* = -\frac{a_{21}}{a_{66}}, \quad a_{22}^* = \frac{a_{11}}{a_{66}}, \quad a_{23}^* = \frac{a_{13}a_{21} - a_{23}a_{11}}{a_{66}}, \quad a_{24}^* = \frac{a_{14}a_{21} - a_{24}a_{11}}{a_{66}}, \quad a_{25}^* = \frac{a_{15}a_{21} - a_{25}a_{11}}{a_{66}},\\
&a_{26}^* = \frac{a_{16}a_{21} - a_{26}a_{11}}{a_{66}}, \quad a_{27}^* = \frac{a_{17}a_{21} - a_{27}a_{11}}{a_{66}}, \quad a_{28}^* = \frac{a_{18}a_{21}}{a_{66}}, \quad a_{29}^* = -\frac{a_{28}a_{11}}{a_{66}},\\
&a_{31}^* = \frac{1}{a_{31}}, \quad a_{32}^* = -\frac{a_{32}}{a_{31}}, \quad a_{33}^* = -\frac{a_{33}}{a_{31}}, \quad a_{34}^* = -\frac{a_{34}}{a_{31}}.
\end{aligned} \tag{16}$$

Substituting Eq. (15) into Eq. (11, 12) yields

$$\begin{aligned}
M_x &= b_{11}^* N_x + b_{12}^* N_y + b_{13}^* \phi_{x,x} + b_{14}^* \phi_{y,y} + b_{15}^* w_{,xx} + b_{16}^* w_{,yy} + b_{17}^* \phi_1^{\mathrm{p}}\\
&\quad + b_{18}^* \phi_1^{sx} + b_{19}^* \phi_1^{sy} + b_{17} \phi_2^{\mathrm{p}} + b_{18} \phi_2^{sx},\\
M_y &= b_{21}^* N_x + b_{22}^* N_y + b_{23}^* \phi_{x,x} + b_{24}^* \phi_{y,y} + b_{25}^* w_{,xx} + b_{26}^* w_{,yy} + b_{27}^* \phi_1^{\mathrm{p}}\\
&\quad + b_{28}^* \phi_1^{sx} + b_{29}^* \phi_1^{sy} + b_{27} \phi_2^{\mathrm{p}} + b_{28} \phi_2^{sy},\\
M_{xy} &= b_{31}^* N_{xy} + b_{32}^* \phi_{x,y} + b_{33}^* \phi_{y,x} + b_{34}^* w_{,xy},\\
P_x &= c_{11}^* N_x + c_{12}^* N_y + c_{13}^* \phi_{x,x} + c_{14}^* \phi_{y,y} + c_{15}^* w_{,xx} + c_{16}^* w_{,yy} + c_{17}^* \phi_1^{\mathrm{p}}\\
&\quad + c_{18}^* \phi_1^{sx} + c_{19}^* \phi_1^{sy} + c_{17} \phi_4^{\mathrm{p}} + c_{18} \phi_4^{sx},\\
P_y &= c_{21}^* N_x + c_{22}^* N_y + c_{23}^* \phi_{x,x} + c_{24}^* \phi_{y,y} + c_{25}^* w_{,xx} + c_{26}^* w_{,yy} + c_{27}^* \phi_1^{\mathrm{p}}\\
&\quad + c_{28}^* \phi_1^{sx} + c_{29}^* \phi_1^{sy} + c_{27} \phi_4^{\mathrm{p}} + c_{28} \phi_4^{sy},\\
P_{xy} &= c_{31}^* N_{xy} + c_{32}^* \phi_{x,y} + c_{33}^* \phi_{y,x} + c_{34}^* w_{,xy}
\end{aligned} \tag{17}$$

where

$$\begin{aligned}
&b_{11}^* = b_{11}a_{11}^* + b_{12}a_{21}^*, \quad b_{12}^* = b_{11}a_{12}^* + b_{12}a_{22}^*, \quad b_{13}^* = b_{11}a_{13}^* + b_{12}a_{23}^* + b_{13},\\
&b_{14}^* = b_{11}a_{14}^* + b_{12}a_{24}^* + b_{14}, \quad b_{15}^* = b_{11}a_{15}^* + b_{12}a_{25}^* + b_{15}, \quad b_{16}^* = b_{11}a_{16}^* + b_{12}a_{26}^* + b_{16},\\
&b_{17}^* = b_{11}a_{17}^* + b_{12}a_{27}^*, \quad b_{18}^* = b_{11}a_{18}^* + b_{12}a_{28}^*, \quad b_{19}^* = b_{11}a_{19}^* + b_{12}a_{29}^*,\\
&b_{21}^* = b_{21}a_{11}^* + b_{22}a_{21}^*, \quad b_{22}^* = b_{21}a_{12}^* + b_{22}a_{22}^*, \quad b_{23}^* = b_{21}a_{13}^* + b_{22}a_{23}^* + b_{23},\\
&b_{24}^* = b_{21}a_{14}^* + b_{22}a_{24}^* + b_{24}, \quad b_{25}^* = b_{21}a_{15}^* + b_{22}a_{25}^* + b_{25}, \quad b_{26}^* = b_{21}a_{16}^* + b_{22}a_{26}^* + b_{26},\\
&b_{27}^* = b_{21}a_{17}^* + b_{22}a_{27}^*, \quad b_{28}^* = b_{21}a_{18}^* + b_{22}a_{28}^*, \quad b_{29}^* = b_{21}a_{19}^* + b_{22}a_{29}^*,\\
&b_{31}^* = b_{31}a_{31}^*, \quad b_{32}^* = b_{31}a_{32}^* + b_{32}, \quad b_{33}^* = b_{31}a_{33}^* + b_{33}, \quad b_{34}^* = b_{31}a_{34}^* + b_{34},\\
&c_{11}^* = c_{11}a_{11}^* + c_{12}a_{21}^*, \quad c_{12}^* = c_{11}a_{12}^* + c_{12}a_{22}^*, \quad c_{13}^* = c_{11}a_{13}^* + c_{12}a_{23}^* + c_{13},\\
&c_{14}^* = c_{11}a_{14}^* + c_{12}a_{24}^* + c_{14}, \quad c_{15}^* = c_{11}a_{15}^* + c_{12}a_{25}^* + c_{15}, \quad c_{16}^* = c_{11}a_{16}^* + c_{12}a_{26}^* + c_{16},\\
&c_{17}^* = c_{11}a_{17}^* + c_{12}a_{27}^*, \quad c_{18}^* = c_{11}a_{18}^* + c_{12}a_{28}^*, \quad c_{19}^* = c_{11}a_{19}^* + c_{12}a_{29}^*,\\
&c_{21}^* = c_{21}a_{11}^* + c_{22}a_{21}^*, \quad c_{22}^* = c_{21}a_{12}^* + c_{22}a_{22}^*, \quad c_{23}^* = c_{21}a_{13}^* + c_{22}a_{23}^* + c_{23},\\
&c_{24}^* = c_{21}a_{14}^* + c_{22}a_{24}^* + c_{24}, \quad c_{25}^* = c_{21}a_{15}^* + c_{22}a_{25}^* + c_{25}, \quad c_{26}^* = c_{21}a_{16}^* + c_{22}a_{26}^* + c_{26},\\
&c_{27}^* = c_{21}a_{17}^* + c_{22}a_{27}^*, \quad c_{28}^* = c_{21}a_{18}^* + c_{22}a_{28}^*, \quad c_{29}^* = c_{21}a_{19}^* + c_{22}a_{29}^*,\\
&c_{31}^* = c_{31}a_{31}^*, \quad c_{32}^* = c_{31}a_{32}^* + c_{32}, \quad c_{33}^* = c_{31}a_{33}^* + c_{33}, \quad c_{34}^* = c_{31}a_{34}^* + c_{34}.
\end{aligned} \tag{18}$$

The nonlinear equilibrium equations of an imperfect FGM plate on elastic foundations based on Reddy's third-order shear deformation theory are [7,37,38]

$$N_{x,x} + N_{xy,y} = 0, \tag{19.1}$$
$$N_{xy,x} + N_{y,y} = 0, \tag{19.2}$$
$$Q_{x,x} + Q_{y,y} - 3\lambda\left(R_{x,x} + R_{y,y}\right) + \lambda\left(P_{x,xx} + 2P_{xy,xy} + P_{y,yy}\right) + N_x\left(w_{,xx} + w^*_{,xx}\right) + 2N_{xy}\left(w_{,xy} + w^*_{,xy}\right) + N_y\left(w_{,yy} + w^*_{,yy}\right) + q - K_1 w + K_2\nabla^2 w = 0, \tag{19.3}$$
$$M_{x,x} + M_{xy,y} - Q_x + 3\lambda R_x - \lambda\left(P_{x,x} + P_{xy,y}\right) = 0, \tag{19.4}$$
$$M_{xy,x} + M_{y,y} - Q_y + 3\lambda R_y - \lambda\left(P_{xy,x} + P_{y,y}\right) = 0 \tag{19.5}$$

where q is a uniform transversal force.

By putting

$$N_x = f_{,yy}, \quad N_y = f_{,xx}, \quad N_{xy} = -f_{,xy}, \tag{20}$$

it is easy to see that the first two equations (19.1) and (19.2) are automatically satisfied, and the three other equations become

$$\begin{aligned}
&M_{x,xx} + 2M_{xy,xy} + M_{y,yy} + f_{,yy}\left(w_{,xx} + w^*_{,xx}\right) - 2f_{,xy}\left(w_{,xy} + w^*_{,xy}\right) + f_{,xx}\left(w_{,\mathrm{yy}} + w^*_{,\mathrm{yy}}\right) \\
&\quad + q - K_1 w + K_2\nabla^2 w = 0, \\
&M_{x,x} + M_{xy,y} - Q_x + 3\lambda R_x - \lambda\left(P_{x,x} + P_{xy,y}\right) = 0, \\
&M_{xy,x} + M_{y,y} - Q_y + 3\lambda R_y - \lambda\left(P_{xy,x} + P_{y,y}\right) = 0.
\end{aligned} \tag{21}$$

Substituting the expressions of M_{ij}, P_{ij} from Eq. (17) and Q_x, Q_y, R_x, R_y from Eq. (13.1) into Eq. (21), we obtain

$$\begin{aligned}
&b^*_{12}f_{,xxxx} + \left(b^*_{11} + b^*_{22} - 2b^*_{31}\right)f_{,xxyy} + b^*_{21}f_{,yyyy} + b^*_{13}\phi_{x,xxx} + \left(b^*_{23} + 2b^*_{32}\right)\phi_{x,xyy} \\
&\quad + \left(b^*_{14} + 2b^*_{33}\right)\phi_{y,xxy} + b^*_{24}\phi_{y,yyy} + b^*_{15}w_{,xxxx} + \left(b^*_{16} + b^*_{25} + 2b^*_{34}\right)w_{,xxyy} + b^*_{26}w_{,yyyy} \\
&\quad + f_{,yy}\left(w_{,xx} + w^*_{,xx}\right) - 2f_{,xy}\left(w_{,xy} + w^*_{,xy}\right) + f_{,xx}\left(w_{,yy} + w^*_{,yy}\right) + q - K_1 w + K_2\nabla^2 w = 0,
\end{aligned} \tag{22}$$

$$\begin{aligned}
&\left(b^*_{11} - b^*_{31}\right)f_{,xyy} + b^*_{12}f_{,xxx} + b^*_{13}\phi_{x,xx} + \left(b^*_{14} + b^*_{33}\right)\phi_{y,xy} + b^*_{32}\phi_{x,yy} + b^*_{15}w_{,xxx} + \left(b^*_{16} + b^*_{34}\right)w_{,xyy} \\
&\quad - \lambda\left[\left(c^*_{11} - c^*_{31}\right)f_{,xyy} + c^*_{12}f_{,xxx} + c^*_{13}\phi_{x,xx} + \left(c^*_{14} + c^*_{33}\right)\phi_{y,xy}\right. \\
&\quad \left. + c^*_{32}\phi_{x,yy} + c^*_{15}w_{,xxx} + \left(c^*_{16} + c^*_{34}\right)w_{,xyy}\right] - d_{11}\phi_x - d_{12}w_{,x} + 3\lambda\left(e_{11}\phi_x + e_{12}w_{,x}\right) = 0,
\end{aligned} \tag{23}$$

$$\begin{aligned}
&\left(b^*_{22} - b^*_{31}\right)f_{,xxy} + b^*_{21}f_{,yyy} + \left(b^*_{23} + b^*_{32}\right)\phi_{x,xy} + b^*_{33}\phi_{y,xx} + b^*_{24}\phi_{y,yy} + \left(b^*_{25} + b^*_{34}\right)w_{,xxy} + b^*_{26}w_{,yyy} \\
&\quad - \lambda\left[\left(c^*_{22} - c^*_{31}\right)f_{,xxy} + c^*_{21}f_{,yyy} + \left(c^*_{23} + c^*_{32}\right)\phi_{x,xy} + c^*_{33}\phi_{y,xx}\right. \\
&\quad \left. + c^*_{24}\phi_{y,yy} + \left(c^*_{25} + c^*_{34}\right)w_{,xxy} + c^*_{26}w_{,yyy}\right] - d_{21}\phi_y - d_{22}w_{,y} + 3\lambda\left(e_{21}\phi_y + e_{22}w_{,y}\right) = 0.
\end{aligned} \tag{24}$$

The three equations (22), (23) and (24) include four unknown functions w, ϕ_x, ϕ_y, and f, so it is necessary to find the fourth equation relating to these functions by using the compatibility equation (7). For this aim, substituting the expressions of Eq. (15) into Eq. (7), one can write

$$\begin{aligned}
&a^*_{22}f_{,xxxx} + \left(a^*_{12} + a^*_{21} + a^*_{31}\right)f_{,xxyy} + a^*_{11}f_{,yyyy} + a^*_{23}\phi_{x,xxx} + \left(a^*_{13} - a^*_{32}\right)\phi_{x,xyy} + \left(a^*_{24} - a^*_{33}\right)\phi_{y,xxy} \\
&\quad + a^*_{14}\phi_{y,yyy} + a^*_{25}w_{,xxxx} + \left(a^*_{15} + a^*_{26} - a^*_{34}\right)w_{,xxyy} + a^*_{16}w_{,yyyy} \\
&\quad - w^2_{,xy} + w_{,xx}w_{,yy} + w_{,xx}w^*_{,yy} - 2w_{,xy}w^*_{,xy} + w^*_{,xx}w_{,yy} = 0.
\end{aligned} \tag{25}$$

Equations (22)–(25) are four nonlinear and governing equations in terms of four dependent unknown functions w, ϕ_x, ϕ_y, and f. They are used to investigate the buckling and postbuckling of imperfect ES-FGM plates subjected to mechanical loads or thermal loads or thermo-mechanical loads and resting on elastic foundations. It is obvious that this system of equations is more complex than the one established by using the classical plate theory or the nonlinear stability analysis of un-stiffened FGM plates. However, the higher-order theories (including Reddy's third-order shear deformation theory) can represent better the kinematic behavior and may not require shear correction factors. This is also the main reason why these theories are used to investigate the nonlinear buckling and postbuckling of thicker FGM plates.

4 Boundary conditions and Galerkin method

In this paper, three cases of boundary conditions will be considered as follows [4,23,37,38]:

Case (**1**) Four edges of the plate are simply supported and freely movable (FM), i.e.,

$$\begin{aligned} &w = \phi_y = N_{xy} = M_x = P_x = 0, \quad N_x = N_{xo} \text{ at } x = 0, a, \\ &w = \phi_x = N_{xy} = M_y = P_y = 0, \quad N_y = N_{yo} \text{ at } y = 0, b. \end{aligned} \tag{26}$$

Case (**2**) Four edges of the plate are simply supported and immovable (IM), i.e.,

$$\begin{aligned} &w = u = \phi_y = M_x = P_x = 0, \quad N_x = N_{xo} \text{ at } x = 0, a, \\ &w = v = \phi_x = M_y = P_y = 0, \quad N_y = N_{yo} \text{ at } y = 0, b. \end{aligned} \tag{27}$$

Case (**3**) Four edges of the plate are simply supported. Uniaxial loads are applied in the direction of the x-coordinate. The edges $x = 0, x = a$ are considered freely movable, the remaining two edges being unloaded and immovable. The boundary conditions, for this case, are

$$\begin{aligned} &w = \phi_y = N_{xy} = M_x = P_x = 0, \quad N_x = N_{xo} \text{ at } x = 0, a, \\ &w = v = \phi_x = M_y = P_y = 0, \quad N_y = N_{yo} \text{ at } y = 0, b \end{aligned} \tag{28}$$

where N_{x0}, N_{y0} are pre-buckling force resultants in the x- and y-directions for case (1) and the first of case (3), and they are fictitious compressive edge loads rendering the immovable edges for case (2) and the second of case (3).

The analytical solution of the system of Eqs. (22)–(25) satisfying the boundary conditions can be found in the form

$$\begin{aligned} w &= W \sin\alpha x \sin\beta y,\ w^* = \xi h \sin\alpha x \sin\beta y, \\ f &= F_1 \cos 2\alpha x + F_2 \cos 2\beta y + F_3 \sin\alpha x \sin\beta y + \frac{1}{2}N_{x0}y^2 + \frac{1}{2}N_{y0}x^2, \\ \phi_x &= \Phi_1 \cos\alpha x \sin\beta y,\ \phi_y = \Phi_2 \sin\alpha x \cos\beta y \end{aligned} \tag{29}$$

where $\alpha = \frac{m\pi}{a}$, $\beta = \frac{n\pi}{b}$ and m, n are numbers of half waves in the x- and y-direction, respectively, and the coefficient $\xi \in [0, 1]$ is an imperfection size of the plate.

By setting Eq. (29) into Eq. (25) and carrying out some calculations, the coefficients $F_i (i = 1{-}3)$ are determined as

$$\begin{aligned} F_1 &= \frac{\beta^2}{32\alpha^2 a_{22}^*} W\left(W + 2\xi h\right),\ F_2 = \frac{\alpha^2}{32\beta^2 a_{11}^*} W\left(W + 2\xi h\right), \\ F_3 &= -\frac{a_{23}^*\alpha^3 + \left(a_{13}^* - a_{32}^*\right)\alpha\beta^2}{a_{22}^*\alpha^4 + \left(a_{12}^* + a_{21}^* + a_{31}^*\right)\alpha^2\beta^2 + a_{11}^*\beta^4}\Phi_1 - \frac{\left(a_{24}^* - a_{33}^*\right)\alpha^2\beta + a_{14}^*\beta^3}{a_{22}^*\alpha^4 + \left(a_{12}^* + a_{21}^* + a_{31}^*\right)\alpha^2\beta^2 + a_{11}^*\beta^4}\Phi_2 \\ &\quad - \frac{a_{25}^*\alpha^4 + \left(a_{15}^* + a_{26}^* - a_{34}^*\right)\alpha^2\beta^2 + a_{16}^*\beta^4}{a_{22}^*\alpha^4 + \left(a_{12}^* + a_{21}^* + a_{31}^*\right)\alpha^2\beta^2 + a_{11}^*\beta^4} W. \end{aligned} \tag{30}$$

Substituting the expressions in Eq. (29) into Eqs. (22), (23) and (24), then applying Galerkin method for the resulting equations, we obtain

$$\begin{aligned} &l_{11}W + l_{12}\Phi_1 + l_{13}\Phi_2 + l_{14}\Phi_1\left(W + \xi h\right) + l_{15}\Phi_2\left(W + \xi h\right) + s_1 W\left(W + \xi h\right) \\ &\quad + s_2 W\left(W + 2\xi h\right) + s_3 W\left(W + \xi h\right)\left(W + 2\xi h\right) + s_4 q - \left(N_{x0}\alpha^2 + N_{y0}\beta^2\right)\left(W + \xi h\right) = 0, \quad (31) \\ &l_{21}W + l_{22}\Phi_1 + l_{23}\Phi_2 + s_5 W\left(W + 2\xi h\right) = 0, \quad (32) \\ &l_{31}W + l_{32}\Phi_1 + l_{33}\Phi_2 + s_6 W\left(W + 2\xi h\right) = 0, \quad (33) \end{aligned}$$

in which $l_{ij}, s_k (k = 1{-}6)$ are determined in "Appendix II."

From Eqs. (32) and (33), we obtain the following expressions:

$$\Phi_1 = \frac{l_{23}l_{31} - l_{21}l_{33}}{l_{22}l_{33} - l_{23}l_{32}} W + \frac{l_{23}s_6 - l_{33}s_5}{l_{22}l_{33} - l_{23}l_{32}} W\,(W + 2\xi h)\,,$$
$$\Phi_2 = \frac{l_{32}l_{21} - l_{22}l_{31}}{l_{22}l_{33} - l_{23}l_{32}} W + \frac{l_{32}s_5 - l_{22}s_6}{l_{22}l_{33} - l_{23}l_{32}} W\,(W + 2\xi h)\,. \tag{34}$$

Substituting Φ_1, Φ_2 from Eq. (34) into Eq. (31) yields the following expressions:

$$\begin{aligned}
&\left(l_{11} + l_{12}\frac{l_{23}l_{31} - l_{21}l_{33}}{l_{22}l_{33} - l_{23}l_{32}} + l_{13}\frac{l_{32}l_{21} - l_{22}l_{31}}{l_{22}l_{33} - l_{23}l_{32}}\right) W \\
&+ \left(s_1 + l_{14}\frac{l_{23}l_{31} - l_{21}l_{33}}{l_{22}l_{33} - l_{23}l_{32}} + l_{15}\frac{l_{32}l_{21} - l_{22}l_{31}}{l_{22}l_{33} - l_{23}l_{32}}\right) W\,(W + \xi h) \\
&+ \left(s_2 + l_{12}\frac{l_{23}s_6 - l_{33}s_5}{l_{22}l_{33} - l_{23}l_{32}} + l_{13}\frac{l_{32}s_5 - l_{22}s_6}{l_{22}l_{33} - l_{23}l_{32}}\right) W\,(W + 2\xi h) \\
&+ \left(s_3 + l_{14}\frac{l_{23}s_6 - l_{33}s_5}{l_{22}l_{33} - l_{23}l_{32}} + l_{15}\frac{l_{32}s_5 - l_{22}s_6}{l_{22}l_{33} - l_{23}l_{32}}\right) W\,(W + \xi h)\,(W + 2\xi h) \\
&+ s_4 q - \left(N_{x0}\alpha^2 + N_{y0}\beta^2\right)(W + \xi h) = 0.
\end{aligned} \tag{35}$$

The nonlinear Eq. (35) is used to determine the buckling loads and to analyze postbuckling load–deflection curves of imperfect ES-FGM plates subjected to mechanical compressive loads or thermal loads or thermo-mechanical loads taking into account elastic foundations.

5 Mechanical stability analysis

Consider a rectangular imperfect ES-FGM plate being simply supported at four edges and freely movable in the plane [Case (1)]. The plate is subjected to the in-plane compressive loads F_x and F_y uniformly distributed along the edges $x = 0, a$ and $y = 0, b$, respectively.

If $q = 0$, $N_{xo} = -hF_x$, $N_{yo} = -hF_y$ and putting $\eta = \frac{F_y}{F_x}$, $\bar{W} = \frac{W}{h}$, Eq. (35) leads to the load–deflection relation as

$$F_x = \frac{-1}{\alpha^2 + \eta\beta^2}\left[\begin{array}{l}
\dfrac{l_{11} + l_{12}\frac{l_{23}l_{31} - l_{21}l_{33}}{l_{22}l_{33} - l_{23}l_{32}} + l_{13}\frac{l_{32}l_{21} - l_{22}l_{31}}{l_{22}l_{33} - l_{23}l_{32}}}{h}\dfrac{\bar{W}}{\bar{W} + \xi} \\
\quad + \left(s_1 + l_{14}\frac{l_{23}l_{31} - l_{21}l_{33}}{l_{22}l_{33} - l_{23}l_{32}} + l_{15}\frac{l_{32}l_{21} - l_{22}l_{31}}{l_{22}l_{33} - l_{23}l_{32}}\right)\bar{W} \\
\quad + \left(s_2 + l_{12}\frac{l_{23}s_6 - l_{33}s_5}{l_{22}l_{33} - l_{23}l_{32}} + l_{13}\frac{l_{32}s_5 - l_{22}s_6}{l_{22}l_{33} - l_{23}l_{32}}\right)\dfrac{\bar{W}(\bar{W} + 2\xi)}{\bar{W} + \xi} \\
\quad + \left(s_3 + l_{14}\frac{l_{23}s_6 - l_{33}s_5}{l_{22}l_{33} - l_{23}l_{32}} + l_{15}\frac{l_{32}s_5 - l_{22}s_6}{l_{22}l_{33} - l_{23}l_{32}}\right) h\bar{W}\left(\bar{W} + 2\xi\right)
\end{array}\right]. \tag{36}$$

The nonlinear Eq. (36) is used to analyze postbuckling load–deflection curves of imperfect ES-FGM plates subjected to mechanical compressive loads.

If the plate is perfect, i.e., $\xi = 0$, taking $\bar{W} \to 0$, Eq. (36) leads to

$$F_x = \frac{-1}{h\left(\alpha^2 + \eta\beta^2\right)}\left(l_{11} + l_{12}\frac{l_{23}l_{31} - l_{21}l_{33}}{l_{22}l_{33} - l_{23}l_{32}} + l_{13}\frac{l_{32}l_{21} - l_{22}l_{31}}{l_{22}l_{33} - l_{23}l_{32}}\right). \tag{37}$$

Equation (37) is used to determine the critical upper buckling load for a perfect ES-FGM plate.

6 Thermal stability analysis

Suppose that an imperfect ES-FGM plate is simply supported with immovable edges [Case (2)]. So the immovable conditions $u = 0$ at $x = 0$, $x = a$ and $v = 0$ at $y = 0$, $y = b$ are fulfilled in the average sense as [4,22]

$$\int_0^b \int_0^a u_{,x}\mathrm{d}x\mathrm{d}y = 0, \quad \int_0^a \int_0^b v_{,y}\mathrm{d}y\mathrm{d}x = 0. \tag{38}$$

From the relations (6.1) and (15), (16), we obtain the following equations:

$$u_{,x} = a_{11}^* f_{,yy} + a_{12}^* f_{,xx} + a_{13}^* \phi_{x,x} + a_{14}^* \phi_{y,y} + a_{15}^* w_{,xx} + a_{16}^* w_{,yy} + a_{17}^* \phi_1^{\mathrm{p}} + a_{18}^* \phi_1^{sx} + a_{19}^* \phi_1^{sy} - \frac{w_{,x}^2}{2} - w_{,x} w_{,x}^*, \tag{39.1}$$

$$v_{,y} = a_{21}^* f_{,yy} + a_{22}^* f_{,xx} + a_{23}^* \phi_{x,x} + a_{24}^* \phi_{y,y} + a_{25}^* w_{,xx} + a_{26}^* w_{,yy} + a_{27}^* \phi_1^{\mathrm{p}} + a_{28}^* \phi_1^{sx} + a_{29}^* \phi_1^{sy} - \frac{w_{,y}^2}{2} - w_{,y} w_{,y}^*. \tag{39.2}$$

Substituting Eq. (29) into Eq. (39.1), and then into the conditions (38), gives us

$$N_{x0} = \frac{a_{22}^* t_{11} - a_{12}^* t_{21}}{a_{11}^* a_{22}^* - a_{12}^* a_{21}^*} W + \frac{a_{22}^* t_{12} - a_{12}^* t_{22}}{a_{11}^* a_{22}^* - a_{12}^* a_{21}^*} W (W + \xi h) - \frac{a_{22}^* a_{17}^* - a_{12}^* a_{27}^*}{a_{11}^* a_{22}^* - a_{12}^* a_{21}^*} \phi_1^{\mathrm{p}} - \frac{a_{22}^* a_{18}^* - a_{12}^* a_{28}^*}{a_{11}^* a_{22}^* - a_{12}^* a_{21}^*} \phi_1^{sx} - \frac{a_{22}^* a_{19}^* - a_{12}^* a_{29}^*}{a_{11}^* a_{22}^* - a_{12}^* a_{21}^*} \phi_1^{sy}, \tag{40.1}$$

$$N_{y0} = \frac{a_{11}^* t_{21} - a_{21}^* t_{11}}{a_{11}^* a_{22}^* - a_{12}^* a_{21}^*} W + \frac{a_{11}^* t_{22} - a_{21}^* t_{12}}{a_{11}^* a_{22}^* - a_{12}^* a_{21}^*} W (W + \xi h) - \frac{a_{11}^* a_{27}^* - a_{21}^* a_{17}^*}{a_{11}^* a_{22}^* - a_{12}^* a_{21}^*} \phi_1^{\mathrm{p}} - \frac{a_{11}^* a_{28}^* - a_{21}^* a_{18}^*}{a_{11}^* a_{22}^* - a_{12}^* a_{21}^*} \phi_1^{sx} - \frac{a_{11}^* a_{29}^* - a_{21}^* a_{19}^*}{a_{11}^* a_{22}^* - a_{12}^* a_{21}^*} \phi_1^{sy} \tag{40.2}$$

where

$$G_3 = -\frac{a_{23}^* \alpha^3 + \left(a_{13}^* - a_{32}^*\right) \alpha \beta^2}{a_{22}^* \alpha^4 + \left(a_{12}^* + a_{21}^* + a_{31}^*\right) \alpha^2 \beta^2 + a_{11}^* \beta^4}, \; G_4 = -\frac{\left(a_{24}^* - a_{33}^*\right) \alpha^2 \beta + a_{14}^* \beta^3}{a_{22}^* \alpha^4 + \left(a_{12}^* + a_{21}^* + a_{31}^*\right) \alpha^2 \beta^2 + a_{11}^* \beta^4},$$

$$G_5 = -\frac{a_{25}^* \alpha^4 + \left(a_{15}^* + a_{26}^* - a_{34}^*\right) \alpha^2 \beta^2 + a_{16}^* \beta^4}{a_{22}^* \alpha^4 + \left(a_{12}^* + a_{21}^* + a_{31}^*\right) \alpha^2 \beta^2 + a_{11}^* \beta^4},$$

$$G_{10} = G_3 \frac{l_{23} l_{31} - l_{21} l_{33}}{l_{22} l_{33} - l_{23} l_{32}} + G_4 \frac{l_{32} l_{21} - l_{22} l_{31}}{l_{22} l_{33} - l_{23} l_{32}} + G_5, \; G_{11} = G_3 \frac{l_{23} s_6 - l_{33} s_5}{l_{22} l_{33} - l_{23} l_{32}} + G_4 \frac{l_{32} s_5 - l_{22} s_6}{l_{22} l_{33} - l_{23} l_{32}},$$

$$t_{11} = \frac{4 \delta_m \delta_n}{mn\pi^2} \left[a_{13}^* \alpha \left(\frac{l_{23} l_{31} - l_{21} l_{33}}{l_{22} l_{33} - l_{23} l_{32}} \right) + a_{14}^* \beta \left(\frac{l_{32} l_{21} - l_{22} l_{31}}{l_{22} l_{33} - l_{23} l_{32}} \right) + a_{15}^* \alpha^2 + a_{16}^* \beta^2 + \left(a_{11}^* \beta^2 + a_{12}^* \alpha^2\right) G_{10} \right],$$

$$t_{12} = \frac{4 \delta_m \delta_n}{mn\pi^2} \left[a_{13}^* \alpha \left(\frac{l_{23} s_6 - l_{33} s_5}{l_{22} l_{33} - l_{23} l_{32}} \right) + a_{14}^* \beta \left(\frac{l_{32} s_5 - l_{22} s_6}{l_{22} l_{33} - l_{23} l_{32}} \right) + \left(a_{11}^* \beta^2 + a_{12}^* \alpha^2\right) G_{11} \right] + \frac{1}{8} \alpha^2,$$

$$t_{21} = \frac{4 \delta_m \delta_n}{mn\pi^2} \left[a_{23}^* \alpha \left(\frac{l_{23} l_{31} - l_{21} l_{33}}{l_{22} l_{33} - l_{23} l_{32}} \right) + a_{24}^* \beta \left(\frac{l_{32} l_{21} - l_{22} l_{31}}{l_{22} l_{33} - l_{23} l_{32}} \right) + a_{25}^* \alpha^2 + a_{26}^* \beta^2 + \left(a_{21}^* \beta^2 + a_{22}^* \alpha^2\right) G_{10} \right],$$

$$t_{22} = \frac{4 \delta_m \delta_n}{mn\pi^2} \left[a_{23}^* \alpha \left(\frac{l_{23} s_6 - l_{33} s_5}{l_{22} l_{33} - l_{23} l_{32}} \right) + a_{24}^* \beta \left(\frac{l_{32} s_5 - l_{22} s_6}{l_{22} l_{33} - l_{23} l_{32}} \right) + \left(a_{21}^* \beta^2 + a_{22}^* \alpha^2\right) G_{11} \right] + \frac{1}{8} \beta^2. \tag{41}$$

Introducing Eq. (40.1) into Eq. (35), with $q = 0$, we get

$$\frac{\left(a_{22}^* a_{17}^* - a_{12}^* a_{27}^*\right) \alpha^2 + \left(a_{11}^* a_{27}^* - a_{21}^* a_{17}^*\right) \beta^2}{a_{11}^* a_{22}^* - a_{12}^* a_{21}^*} \phi_1^{\mathrm{p}} + \frac{\left(a_{22}^* a_{18}^* - a_{12}^* a_{28}^*\right) \alpha^2 + \left(a_{11}^* a_{28}^* - a_{21}^* a_{18}^*\right) \beta^2}{a_{11}^* a_{22}^* - a_{12}^* a_{21}^*} \phi_1^{sx} + \frac{\left(a_{22}^* a_{19}^* - a_{12}^* a_{29}^*\right) \alpha^2 + \left(a_{11}^* a_{29}^* - a_{21}^* a_{19}^*\right) \beta^2}{a_{11}^* a_{22}^* - a_{12}^* a_{21}^*} \phi_1^{sy}$$

$$= -\left(l_{11} + l_{12} \frac{l_{23} l_{31} - l_{21} l_{33}}{l_{22} l_{33} - l_{23} l_{32}} + l_{13} \frac{l_{32} l_{21} - l_{22} l_{31}}{l_{22} l_{33} - l_{23} l_{32}} \right) \frac{W}{W + \xi h} - \left(s_1 + l_{14} \frac{l_{23} l_{31} - l_{21} l_{33}}{l_{22} l_{33} - l_{23} l_{32}} + l_{15} \frac{l_{32} l_{21} - l_{22} l_{31}}{l_{22} l_{33} - l_{23} l_{32}} - t_1 \alpha^2 - t_3 \beta^2 \right) W$$

$$
\begin{aligned}
&- \left(s_2 + l_{12} \frac{l_{23}s_6 - l_{33}s_5}{l_{22}l_{33} - l_{23}l_{32}} + l_{13} \frac{l_{32}s_5 - l_{22}s_6}{l_{22}l_{33} - l_{23}l_{32}} \right) \frac{W\,(W + 2\xi h)}{W + \xi h} \\
&- \left(s_3 + l_{14} \frac{l_{23}s_6 - l_{33}s_5}{l_{22}l_{33} - l_{23}l_{32}} + l_{15} \frac{l_{32}s_5 - l_{22}s_6}{l_{22}l_{33} - l_{23}l_{32}} - t_2\alpha^2 - t_4\beta^2 \right) W\,(W + 2\xi h)
\end{aligned} \tag{42}
$$

where

$$
t_1 = \frac{a_{22}^* t_{11} - a_{12}^* t_{21}}{a_{11}^* a_{22}^* - a_{12}^* a_{21}^*}, \quad t_2 = \frac{a_{22}^* t_{12} - a_{12}^* t_{22}}{a_{11}^* a_{22}^* - a_{12}^* a_{21}^*}, \quad t_3 = \frac{a_{11}^* t_{21} - a_{21}^* t_{11}}{a_{11}^* a_{22}^* - a_{12}^* a_{21}^*}, \quad t_4 = \frac{a_{11}^* t_{22} - a_{21}^* t_{12}}{a_{11}^* a_{22}^* - a_{12}^* a_{21}^*}. \tag{43}
$$

Equation (42) is used to analyze postbuckling load–deflection curves of imperfect ES-FGM plates subjected to thermal loads on elastic foundations.

6.1 Uniform temperature rise

In this case, the FGM plate is exposed to a temperature environment uniformly raised from initial value T_i to final value T_f and $\Delta T = T_f - T_i = \text{const}$. Then, from Eq. (14), the thermal parameters are defined as $\phi_1^{\mathrm{p}} = hP_1\Delta T$, $\phi_1^{\mathrm{s}x} = h_1P_2\Delta T$, $\phi_1^{\mathrm{s}y} = h_2P_3\Delta T$, where

$$
\begin{aligned}
P_1 &= E_{\mathrm{m}}\alpha_{\mathrm{m}} + \frac{1}{k+1}\left(E_{\mathrm{m}}\alpha_{\mathrm{cm}} + E_{\mathrm{cm}}\alpha_{\mathrm{m}}\right) + \frac{1}{2k+1}E_{\mathrm{cm}}\alpha_{\mathrm{cm}}, \\
P_2 &= E_{\mathrm{c}}\alpha_{\mathrm{c}} + \frac{1}{k_2+1}\left(E_{\mathrm{c}}\alpha_{\mathrm{mc}} + E_{\mathrm{mc}}\alpha_{\mathrm{c}}\right) + \frac{1}{2k_2+1}E_{\mathrm{mc}}\alpha_{\mathrm{mc}}, \\
P_3 &= E_{\mathrm{c}}\alpha_{\mathrm{c}} + \frac{1}{k_3+1}\left(E_{\mathrm{c}}\alpha_{\mathrm{mc}} + E_{\mathrm{mc}}\alpha_{\mathrm{c}}\right) + \frac{1}{2k_3+1}E_{\mathrm{mc}}\alpha_{\mathrm{mc}}.
\end{aligned} \tag{44}
$$

Introducing $\phi_1^{\mathrm{p}}, \phi_1^{\mathrm{s}x}, \phi_1^{\mathrm{s}y}$ into Eq. (42), we obtain the expression of temperature–deflection relation as

$$
\Delta T = \frac{-1}{\bar{\lambda}_1 hP_1 + \bar{\lambda}_2 h_1P_2 + \bar{\lambda}_3 h_2P_3}
\left[
\begin{aligned}
&\left(l_{11} + l_{12}\tfrac{l_{23}l_{31} - l_{21}l_{33}}{l_{22}l_{33} - l_{23}l_{32}} + l_{13}\tfrac{l_{32}l_{21} - l_{22}l_{31}}{l_{22}l_{33} - l_{23}l_{32}} \right) \tfrac{\bar{W}}{\bar{W} + \xi} \\
&+ \left(s_1 + l_{14}\tfrac{l_{23}l_{31} - l_{21}l_{33}}{l_{22}l_{33} - l_{23}l_{32}} + l_{15}\tfrac{l_{32}l_{21} - l_{22}l_{31}}{l_{22}l_{33} - l_{23}l_{32}} - t_1\alpha^2 - t_3\beta^2 \right) h\bar{W} \\
&+ \left(s_2 + l_{12}\tfrac{l_{23}s_6 - l_{33}s_5}{l_{22}l_{33} - l_{23}l_{32}} + l_{13}\tfrac{l_{32}s_5 - l_{22}s_6}{l_{22}l_{33} - l_{23}l_{32}} \right) h\tfrac{\bar{W}(\bar{W} + 2\xi)}{\bar{W} + \xi} \\
&+ \left(s_3 + l_{14}\tfrac{l_{23}s_6 - l_{33}s_5}{l_{22}l_{33} - l_{23}l_{32}} + l_{15}\tfrac{l_{32}s_5 - l_{22}s_6}{l_{22}l_{33} - l_{23}l_{32}} - t_2\alpha^2 - t_4\beta^2 \right) h^2\bar{W}\left(\bar{W} + 2\xi\right)
\end{aligned}
\right] \tag{45}
$$

where

$$
\begin{aligned}
\bar{\lambda}_1 &= \frac{\left(a_{22}^* a_{17}^* - a_{12}^* a_{27}^*\right)\alpha^2 + \left(a_{11}^* a_{27}^* - a_{21}^* a_{17}^*\right)\beta^2}{a_{11}^* a_{22}^* - a_{12}^* a_{21}^*}, \quad \bar{\lambda}_2 = \frac{\left(a_{22}^* a_{18}^* - a_{12}^* a_{28}^*\right)\alpha^2 + \left(a_{11}^* a_{28}^* - a_{21}^* a_{18}^*\right)\beta^2}{a_{11}^* a_{22}^* - a_{12}^* a_{21}^*}, \\
\bar{\lambda}_3 &= \frac{\left(a_{22}^* a_{19}^* - a_{12}^* a_{29}^*\right)\alpha^2 + \left(a_{11}^* a_{29}^* - a_{21}^* a_{19}^*\right)\beta^2}{a_{11}^* a_{22}^* - a_{12}^* a_{21}^*}.
\end{aligned} \tag{46}
$$

If the plate is initially perfect, i.e.,$\xi = 0$, from Eq. (46) taking $\bar{W} \to 0$, we receive the expression of buckling temperature change as

$$
\Delta T = \frac{-\left(l_{11} + l_{12}\frac{l_{23}l_{31} - l_{21}l_{33}}{l_{22}l_{33} - l_{23}l_{32}} + l_{13}\frac{l_{32}l_{21} - l_{22}l_{31}}{l_{22}l_{33} - l_{23}l_{32}} \right)}{\bar{\lambda}_1 hP_1 + \bar{\lambda}_2 h_1P_2 + \bar{\lambda}_3 h_2P_3}. \tag{47}
$$

Note that Eqs. (45) and (47) are explicit expressions of $\Delta T - \bar{W}$ relation and buckling temperature change ΔT, respectively, in case of temperature-independent plate material properties. On the contrary, when the material properties of plates and stiffeners depend on temperature, those equations are implicit expressions. In that case, the postbuckling temperature–deflection curves and critical buckling temperatures will be determined by two iterative algorithms as follows:

Iterative algorithm 1 (For determining the critical buckling temperature)

It is necessary to use Eq. (47) with the following steps:

(a1) Begin at the reference temperature, i.e., at $T_0 = 300$ K, and temperature-independent material properties are found at $T_0 = 300$ K. Using Eq. (47), the buckling thermal load $\Delta T_{\rm cr}^{(1)}$ for the plate of temperature-independent material is determined.
(a2) Using the material properties at $T = T_0 + \Delta T_{\rm cr}^{(1)}$ and updating on the right of Eq. (47), the new buckling thermal load $\Delta T_{\rm cr}^{(2)}$ is obtained.
(a3) Repeat step (a2) until the buckling temperature converges to a prescribed error tolerance ε, i.e., the iterative process is defined as the relative difference between two consecutive solutions: $\left|\frac{\Delta T_{\rm cr}^{(\rm i+1)} - \Delta T_{\rm cr}^{(\rm i)}}{\Delta T_{\rm cr}^{(\rm i)}}\right| \le \varepsilon$.

Iterative algorithm 2 (For determining postbuckling temperature–deflection curves)
It is necessary to use Eq. (45) with the following steps:

(b1) Begin with $W/h = 0$ at a specific point.
(b2) Use iterative procedures (a1)–(a3).
(b3) Specify the new value of W/h, repeat step (b2) until the postbuckling temperature converges to a prescribed error tolerance.
(b4) Repeat steps (b2)–(b3) to obtain the postbuckling curve.

6.2 Nonlinear temperature change across the thickness

Assume that the temperature through thickness is governed by the one-dimensional Fourier equation of steady-state heat conduction:

$$\text{For plate} \quad \frac{\mathrm{d}}{\mathrm{d}z}\left[\kappa_{\rm p}(z)\frac{\mathrm{d}T}{\mathrm{d}z}\right] = 0, \quad T\big|_{z=-h/2} = T_{\rm m}, \quad T\big|_{z=h/2} = T_{\rm c}, \tag{48}$$

$$\text{For } x\text{-direction stiffeners} \quad \frac{\mathrm{d}}{\mathrm{d}z}\left[\kappa_{sx}(z)\frac{\mathrm{d}T}{\mathrm{d}z}\right] = 0, \quad T\big|_{z=h/2} = T_{\rm c}, \quad T\big|_{z=h/2+h_1} = T_{\rm m}, \tag{49}$$

$$\text{For } y\text{-direction stiffeners} \quad \frac{\mathrm{d}}{\mathrm{d}z}\left[\kappa_{sy}(z)\frac{\mathrm{d}T}{\mathrm{d}z}\right] = 0, \quad T\big|_{z=h/2} = T_{\rm c}, \quad T\big|_{z=h/2+h_2} = T_{\rm m} \tag{50}$$

where $T_{\rm m}$ and $T_{\rm c}$ are temperatures at metal-rich and ceramic-rich surfaces, respectively.

By solving Eqs. (48–50) with the mentioned boundary conditions, the solution for the temperature distribution across the plate thickness is

$$T_{\rm p}(z) = T_{\rm m} + \Delta T^* \frac{\sum_{p=0}^{\infty} \frac{1}{kp+1}\left(-\frac{\kappa_{\rm cm}}{\kappa_{\rm m}}\right)^p \left(\frac{2z+h}{2h}\right)^{kp+1}}{\sum_{p=0}^{\infty} \frac{1}{kp+1}\left(-\frac{\kappa_{\rm cm}}{\kappa_{\rm m}}\right)^p}, \tag{51}$$

and the solutions for the temperature distribution across the stiffener thickness are

$$T_{sx}(z) = T_{\rm c} - \Delta T^* \frac{\sum_{p=0}^{\infty} \frac{1}{k_2 p+1}\left(-\frac{\kappa_{\rm mc}}{\kappa_{\rm c}}\right)^p \left(\frac{2z-h}{2h_1}\right)^{k_2 p+1}}{\sum_{p=0}^{\infty} \frac{1}{k_2 p+1}\left(-\frac{\kappa_{\rm mc}}{\kappa_{\rm c}}\right)^p}, \tag{52}$$

$$T_{sy}(z) = T_{\rm c} - \Delta T^* \frac{\sum_{p=0}^{\infty} \frac{1}{k_3 p+1}\left(-\frac{\kappa_{\rm mc}}{\kappa_{\rm c}}\right)^p \left(\frac{2z-h}{2h_2}\right)^{k_3 p+1}}{\sum_{p=0}^{\infty} \frac{1}{k_3 p+1}\left(-\frac{\kappa_{\rm mc}}{\kappa_{\rm c}}\right)^p}, \tag{53}$$

in which $\Delta T^* = T_{\rm c} - T_{\rm m}$ is the temperature change between ceramic surface and metal surface of the plate.

From Eqs. (51–53), we obtain the expressions $\Delta T(z)$ respecting $T_{\rm p}(z)$, $T_{sx}(z)$ and $T_{sy}(z)$. Then, by the same procedure as in the Sect. 6.1, the expressions of the thermal parameter from Eq. (14), in this case, are

$$\phi_1^{\rm p} = hH_{\rm p}\Delta T^*, \quad \phi_1^{sx} = h_1 H_{sx}\Delta T^*, \phi_1^{sy} = h_2 H_{sy}\Delta T^* \tag{54}$$

where

$$H_{\mathrm{p}} = \frac{\sum_{p=0}^{\infty} \frac{1}{kp+1} \left(\frac{-\kappa_{\mathrm{cm}}}{\kappa_{\mathrm{m}}}\right)^{p} \left(\frac{E_{\mathrm{m}}\alpha_{\mathrm{m}}}{kp+2} + \frac{E_{\mathrm{m}}\alpha_{\mathrm{cm}}+E_{\mathrm{cm}}\alpha_{\mathrm{m}}}{kp+k+2} + \frac{E_{\mathrm{cm}}\alpha_{\mathrm{cm}}}{kp+2k+2}\right)}{\sum_{p=0}^{\infty} \frac{1}{kp+1} \left(\frac{-\kappa_{\mathrm{cm}}}{\kappa_{\mathrm{m}}}\right)^{p}},$$

$$H_{sx} = E_{\mathrm{c}}\alpha_{\mathrm{c}} + \frac{E_{\mathrm{c}}\alpha_{\mathrm{mc}} + E_{\mathrm{mc}}\alpha_{\mathrm{c}}}{k_2+1} + \frac{E_{\mathrm{mc}}\alpha_{\mathrm{mc}}}{2k_2+1} - \frac{\sum_{p=0}^{\infty} \frac{1}{k_2 p+1} \left(\frac{-\kappa_{\mathrm{mc}}}{\kappa_{\mathrm{c}}}\right)^{p} \left(\frac{E_{\mathrm{c}}\alpha_{\mathrm{c}}}{k_2 p+2} + \frac{E_{\mathrm{c}}\alpha_{\mathrm{mc}}+E_{\mathrm{mc}}\alpha_{\mathrm{c}}}{k_2 p+k_2+2} + \frac{E_{\mathrm{mc}}\alpha_{\mathrm{mc}}}{k_2 p+2k_2+2}\right)}{\sum_{p=0}^{\infty} \frac{1}{k_2 p+1} \left(\frac{-\kappa_{\mathrm{mc}}}{\kappa_{\mathrm{c}}}\right)^{p}},$$

$$H_{sy} = E_{\mathrm{c}}\alpha_{\mathrm{c}} + \frac{E_{\mathrm{c}}\alpha_{\mathrm{mc}} + E_{\mathrm{mc}}\alpha_{\mathrm{c}}}{k_3+1} + \frac{E_{\mathrm{mc}}\alpha_{\mathrm{mc}}}{2k_3+1} - \frac{\sum_{p=0}^{\infty} \frac{1}{k_3 p+1} \left(\frac{-\kappa_{\mathrm{mc}}}{\kappa_{\mathrm{c}}}\right)^{p} \left(\frac{E_{\mathrm{c}}\alpha_{\mathrm{c}}}{k_3 p+2} + \frac{E_{\mathrm{c}}\alpha_{\mathrm{mc}}+E_{\mathrm{mc}}\alpha_{\mathrm{c}}}{k_3 p+k_3+2} + \frac{E_{\mathrm{mc}}\alpha_{\mathrm{mc}}}{k_3 p+2k_3+2}\right)}{\sum_{p=0}^{\infty} \frac{1}{k_3 p+1} \left(\frac{-\kappa_{\mathrm{mc}}}{\kappa_{\mathrm{c}}}\right)^{p}}. \tag{55}$$

Introducing $\phi_1^{\mathrm{p}}, \phi_1^{sx}, \phi_1^{sy}$ from Eq. (54) into Eq. (42), we will obtain the temperature–deflection implicit relation for an ES-FGM plate with nonlinear temperature change.

In case of temperature-dependent material properties, postbuckling temperature–deflection curves and critical buckling temperatures also will be determined by an above-presented iterative algorithm.

7 Thermo-mechanical stability analysis

Consider an imperfect ES-FGM plate simultaneously acted by a thermal field and a uniaxial compressive loading F_x, uniformly distributed along the edges $x = 0$ and $x = a$. Suppose that the plate is simply supported with movable edges $x = 0, a$, and immovable $y = 0, b$ [Case (3)]. Employing $N_{x0} = -F_x h$ and Eqs. (39.1) and (40.2), we obtain

$$N_{y0} = \frac{a_{21}^*}{a_{22}^*} P_x h + \frac{t_{21}}{a_{22}^*} W + \frac{t_{22}}{a_{22}^*} W (W + \xi h) - \frac{a_{27}^*}{a_{22}^*}\phi_1^{\mathrm{p}} - \frac{a_{28}^*}{a_{22}^*}\phi_1^{sx} - \frac{a_{29}^*}{a_{22}^*}\phi_1^{sy}. \tag{56}$$

Substituting the expressions of $N_{x0} = -F_x h$ and N_{y0}, taking into account the expressions of $\phi_1^{\mathrm{p}}, \phi_1^{sx}, \phi_1^{sy}$ the yields the following expression:

For the plate under uniform temperature rise:

$$F_x = \frac{a_{22}^*}{h\left(a_{21}^*\beta^2 - a_{22}^*\alpha^2\right)} \left[\begin{array}{l} \left(l_{11} + l_{12}\frac{l_{23}l_{31}-l_{21}l_{33}}{l_{22}l_{33}-l_{23}l_{32}} + l_{13}\frac{l_{32}l_{21}-l_{22}l_{31}}{l_{22}l_{33}-l_{23}l_{32}}\right)\frac{\bar{W}}{\bar{W}+\xi} \\ \quad + \left(s_1 + l_{14}\frac{l_{23}l_{31}-l_{21}l_{33}}{l_{22}l_{33}-l_{23}l_{32}} + l_{15}\frac{l_{32}l_{21}-l_{22}l_{31}}{l_{22}l_{33}-l_{23}l_{32}} - \frac{t_{21}}{a_{22}^*}\right) h\bar{W} \\ \quad + h\left(s_2 + l_{12}\frac{l_{23}s_6-l_{33}s_5}{l_{22}l_{33}-l_{23}l_{32}} + l_{13}\frac{l_{32}s_5-l_{22}s_6}{l_{22}l_{33}-l_{23}l_{32}}\right)\frac{\bar{W}(\bar{W}+2\xi)}{(\bar{W}+\xi)} \\ \quad + \left(s_3 + l_{14}\frac{l_{23}s_6-l_{33}s_5}{l_{22}l_{33}-l_{23}l_{32}} + l_{15}\frac{l_{32}s_5-l_{22}s_6}{l_{22}l_{33}-l_{23}l_{32}} - \frac{t_{22}}{a_{22}^*}\right) h^2\bar{W}\left(\bar{W}+2\xi\right) \\ \quad + \frac{s_4}{h(\bar{W}+\xi)}q + \beta^2\left(\frac{a_{27}^*}{a_{22}^*}hP_1 + \frac{a_{28}^*}{a_{22}^*}h_1P_2 + \frac{a_{29}^*}{a_{22}^*}h_2P_3\right)\Delta T \end{array}\right], \tag{57}$$

for the plate under nonlinear temperature change:

$$F_x = \frac{a_{22}^*}{h\left(a_{21}^*\beta^2 - a_{22}^*\alpha^2\right)} \left[\begin{array}{l} \left(l_{11} + l_{12}\frac{l_{23}l_{31}-l_{21}l_{33}}{l_{22}l_{33}-l_{23}l_{32}} + l_{13}\frac{l_{32}l_{21}-l_{22}l_{31}}{l_{22}l_{33}-l_{23}l_{32}}\right)\frac{\bar{W}}{\bar{W}+\xi} \\ \quad + \left(s_1 + l_{14}\frac{l_{23}l_{31}-l_{21}l_{33}}{l_{22}l_{33}-l_{23}l_{32}} + l_{15}\frac{l_{32}l_{21}-l_{22}l_{31}}{l_{22}l_{33}-l_{23}l_{32}} - \frac{t_{21}}{a_{22}^*}\right) h\bar{W} \\ \quad + h\left(s_2 + l_{12}\frac{l_{23}s_6-l_{33}s_5}{l_{22}l_{33}-l_{23}l_{32}} + l_{13}\frac{l_{32}s_5-l_{22}s_6}{l_{22}l_{33}-l_{23}l_{32}}\right)\frac{\bar{W}(\bar{W}+2\xi)}{(\bar{W}+\xi)} \\ \quad + \left(s_3 + l_{14}\frac{l_{23}s_6-l_{33}s_5}{l_{22}l_{33}-l_{23}l_{32}} + l_{15}\frac{l_{32}s_5-l_{22}s_6}{l_{22}l_{33}-l_{23}l_{32}} - \frac{t_{22}}{a_{22}^*}\right) h^2\bar{W}\left(\bar{W}+2\xi\right) \\ \quad + \frac{s_4}{h(\bar{W}+\xi)}q + \beta^2\left(\frac{a_{27}^*}{a_{22}^*}hH_{\mathrm{p}} + \frac{a_{28}^*}{a_{22}^*}h_1H_{sx} + \frac{a_{29}^*}{a_{22}^*}h_2H_{sy}\right)\Delta T^* \end{array}\right]. \tag{58}$$

Equations (57) and (58) are employed to trace postbuckling load–deflection curves of the imperfect ES-FGM plates subjected to the combined mechanical and thermal loads.

8 Numerical results and discussion

8.1 Validation of the present approach

As part of the validation of the present approach, three comparisons are carried out.

First comparison Consider a simply supported un-stiffened isotropic square plate ($a = b$) without elastic foundations subjected to loads as follows:

– Uniaxial compressive load along x-axis with the nondimensional critical buckling loads

$$\bar{N}_1 = \frac{-F_x h b^2}{D};$$

– Uniaxial compressive load along y-axis with the nondimensional critical buckling loads

$$\bar{N}_2 = \frac{-F_y h b^2}{D};$$

– Biaxial compressive loads with the nondimensional critical buckling loads

$$\bar{N} = \bar{N}_1 + \bar{N}_2,$$

in which $D = \frac{Eh^3}{12(1-\nu^2)}$ and F_x is given by Eq. (37) with $\eta = 0$, F_y is determined from Eq. (35) with $q = 0$, $F_x = 0$, $\xi = 0$, $N_{y0} = -hF_y$.

Table 1 shows the present results compared with those of Huu-Tai Thai and Dong-Ho Choi [41] based on refined plate theory (RPT).

As can be observed, the present results coincide with those of Ref. [41].

Second comparison Consider an un-stiffened FGM plate without elastic foundations with parameters [2] $E_m = 70\,\text{GPa}$, $E_c = 380\,\text{GPa}$, $\nu = 0.3$, $a/b = 0.5$, $m = n = 1$.

Table 1 Comparison of nondimensional critical buckling loads with the results of Ref. [41] for un-stiffened isotropic plates without elastic foundations

a/b	b/h	Work	$\bar{N}_1$	$\bar{N}_2$	$\bar{N}$
1	10	Ref. [41]	3.7866	3.7866	1.8933
		Present	3.7866*	3.7866	1.8933
	20	Ref. [41]	3.2653	3.2653	1.6327
		Present	3.2653	3.2653	1.6327
	30	Ref. [41]	2.6586	2.6586	1.3293
		Present	2.6586	2.6586	1.3293
	40	Ref. [41]	1.9550	1.9550	1.0566
		Present	1.9550 (2,1)	1.9550 (1,2)	1.0567
1.5	10	Ref. [41]	4.0253	2.0048	1.3879
		Present	4.0253 (2,1)	2.0048	1.3879
	20	Ref. [41]	3.3077	1.7946	1.2424
		Present	3.3077 (2,1)	1.7946	1.2424
	30	Ref. [41]	2.5545	1.5285	1.0582
		Present	2.5545 (2,1)	1.5285	1.0582
	40	Ref. [41]	1.9421	1.2670	0.8772
		Present	1.9421 (2,1)	1.2670	0.8772
2	10	Ref. [41]	3.7866	1.5093	1.2075
		Present	3.7866 (2,1)	1.5093	1.2075
	20	Ref. [41]	3.2653	1.3697	1.0958
		Present	3.2653 (2,1)	1.3697	1.0958
	30	Ref. [41]	2.5839	1.1873	0.9498
		Present	2.5839 (3,1)	1.1873	0.9498
	40	Ref. [41]	1.9230	1.0015	0.8012
		Present	1.9230 (3,1)	1.0015	0.8012

* The remaining cases are taken with mode $(m, n) = (1, 1)$.

Table 2 Comparison of the critical buckling load F_x^* with the results of [2] for un-stiffened FGM plates without elastic foundations

η	Theory	$b/h = 10$	$b/h = 20$	$b/h = 40$	$b/h = 60$	$b/h = 80$	$b/h = 100$
0	CPT [2]	267.48	33.435	4.1794	1.2383	0.5224	0.2675
	TSDT [2]	239.15	32.472	4.1486	1.2343	0.5215	0.2672
	Present	239.15	32.472	4.1486	1.2343	0.5215	0.2672
1	CPT [2]	213.99	26.748	3.4353	0.9907	0.4179	0.2140
	TSDT [2]	191.32	25.978	3.3189	0.9879	0.4172	0.2137
	Present	191.32	25.978	3.3189	0.9874	0.4172	0.2137
−1	CPT[2]	356.64	44.580	5.5725	1.6511	0.6966	0.3566
	TSDT [2]	318.86	43.296	5.5315	1.6457	0.6953	0.3562
	Present	318.86	43.296	5.5315	1.6457	0.6953	0.3562

Table 3 Comparison of the critical buckling load F_x^{cr}(Pa) ($\times 10^8$) with the results of [30] for un-stiffened and stiffened FGM plates without elastic foundations

k	Un-stiffened		Stiffened	
	Ref. [23]	Present	Ref. [23]	Present
0.2	0.3204 (1,1)	0.32033 (1,1)	1.3503 (1,1)	1.3495 (1,1)
1	0.1948 (1,1)	0.19475 (1,1)	1.1552 (1,1)	1.1545 (1,1)
5	0.1285 (1,1)	0.12850 (1,1)	1.0309 (1,1)	1.0302 (1,1)
10	0.1171 (1,1)	0.11705 (1,1)	1.0236 (1,1)	1.0229 (1,1)

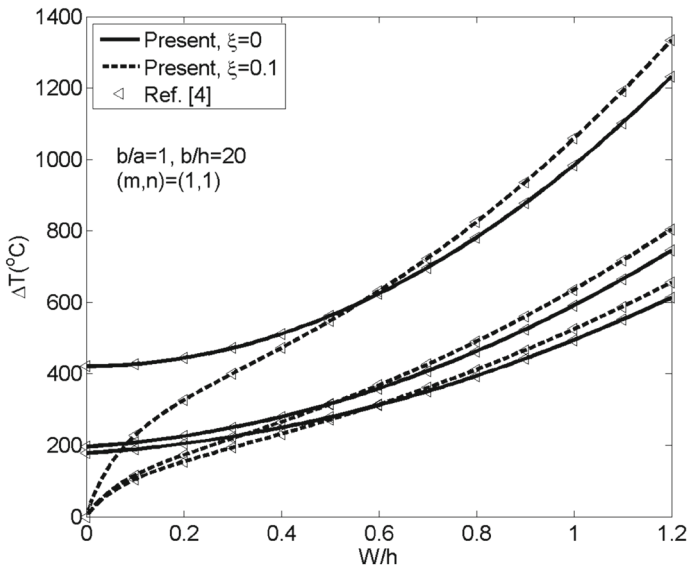

Fig. 2 Comparison of the effects of the volume fraction index on the postbuckling of un-stiffened FGM plates without elastic foundations under uniform temperature rise

The results of the critical buckling load $F_x^* = bhF_x^{\mathrm{cr}}$,with F_x^{cr} given by Eq. (37), are compared with those of Shariat and Eslami [2] based on TSDT (Table 2). It can be seen that the present solutions are in close agreement with TSDT [2].

Third comparison Table 3 presents the comparison on the results of the critical buckling load F_x^{cr} of the FGM plate [given by Eq. (37)], with the results of Bich et al. [30] based on CPT. The input parameters of the FGM plate are taken to be $a = b = 1.5\,\mathrm{m}$, $h = 0.008\,\mathrm{m}$, $h_1 = h_2 = 30 \times 10^{-3}\,\mathrm{m}$, $b_1 = b_2 = 3 \times 10^{-3}\,\mathrm{m}$, $d_1 = d_2 = 0.15\,\mathrm{m}$, $E_{\mathrm{m}} = 70\,\mathrm{GPa}$, $E_{\mathrm{c}} = 380\,\mathrm{GPa}$, $\nu = 0.3$.

As can be seen, a very good agreement is obtained in this comparison.

Fourth comparison Figure 2 illustrates the present results with the results of Duc and Tung [4] for un-stiffened FGM plates without elastic foundations and under the uniform temperature rise based on the TSDT with parameters $E_{\mathrm{c}} = 380 \times 10^9\,\mathrm{Pa}$, $\alpha_{\mathrm{c}} = 7.4 \times 10^{-6}\,^{\circ}\mathrm{C}^{-1}$, $E_{\mathrm{m}} = 70 \times 10^9\,\mathrm{Pa}$, $\alpha_{\mathrm{m}} = 23 \times 10^{-6}\,^{\circ}\mathrm{C}^{-1}$, $\nu = 0.3$.

Table 4 Temperature-dependent coefficients E (in Pa), α (in K^{-1}), and κ(in $W\,mK^{-1}$) for ceramics and metals (from Reddy and Chin [42])

Materials	Properties	P_0	P_{-1}	P_1	P_2	P_3
Silicon nitride	E	348.43e+9	0	−3.070e−4	2.160e−7	−8.946e−11
	α	5.8723e−6	0	9.095e−4	0	0
	κ	13.723	0	−1.032e−3	5.466e−7	−7.876e−11
Stainless steel	E	201.04e+9	0	3.079e−4	−6.534e − 7	0
	α	12.330e−6	0	8.086e−4	0	0
	κ	15.379	0	−1.264e−3	2.092e−6	−7.223e−10

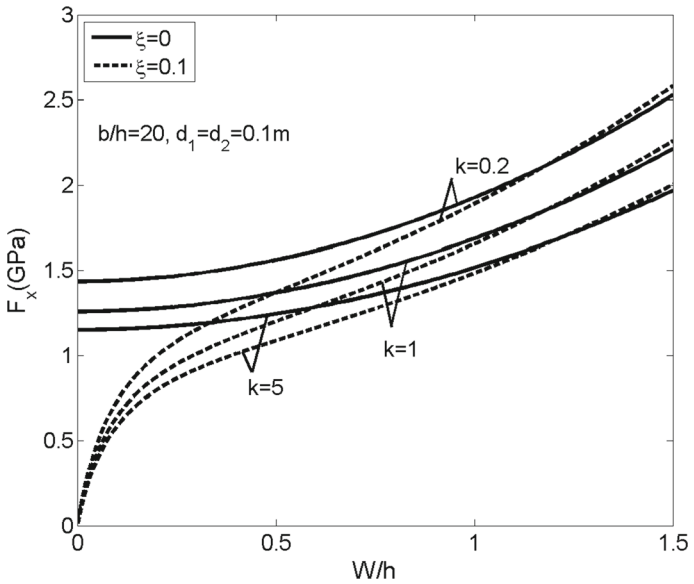

Fig. 3 Effect of the volume fraction index k on the postbuckling behavior of ES-FGM plates under uniaxial compression

As can be observed, a good agreement can be witnessed.

8.2 Numerical results for ES-FGM plates on elastic foundations

Numerical results are presented in this Section for FGM plates made from a mixture of ceramic (Silicon nitride Si_3N_4) and metal (Stainless steel SUS304) reinforced by FGM stiffeners made from Si_3N_4/ SUS304. The geometric property of the plate is $b = 1\,\text{m}$, and the geometric properties of the stiffeners are $b_1 = b_2 = 0.005m, h_1 = h_2 = 0.02\,\text{m}, k_2 = k_3 = 1/k$. The elastic foundation parameters are used as $K_1 = 5 \times 10^7\,\text{N/m}^3$, $K_2 = 10^5\,\text{N/m}$ (except in Sect. 8.2.4). The buckling load is minimum corresponding to the buckling mode $(m, n) = (1, 1)$.

The material properties, such as Young's modulus E, thermal expansion coefficient α and thermal conductivity κ, can be expressed as a nonlinear function of temperature (from Reddy and Chin [42]) as

$$P = P_0\left(P_{-1}T^{-1} + 1 + P_1T + P_2T^2 + P_3T^3\right) \tag{59}$$

in which $T = T_0 + \Delta T$ and $T_0 = 300\,\text{K}$ (room temperature), P_0, P_{-1}, P_2, P_1 and P_3 are the coefficients of temperature T (K) and are unique to the constituent materials (Table 4). Poisson's ratio ν is assumed to be a constant, and $\nu = 0.28$.

8.2.1 Effect of volume fraction indices k, k_2, k_3

Figure 3 illustrates the effect of volume fraction index k ($k_2 = k_3 = 1/k$) on the postbuckling $F_x - W/h$ curves of ES-FGM plates on an elastic foundation under uniaxial compression.

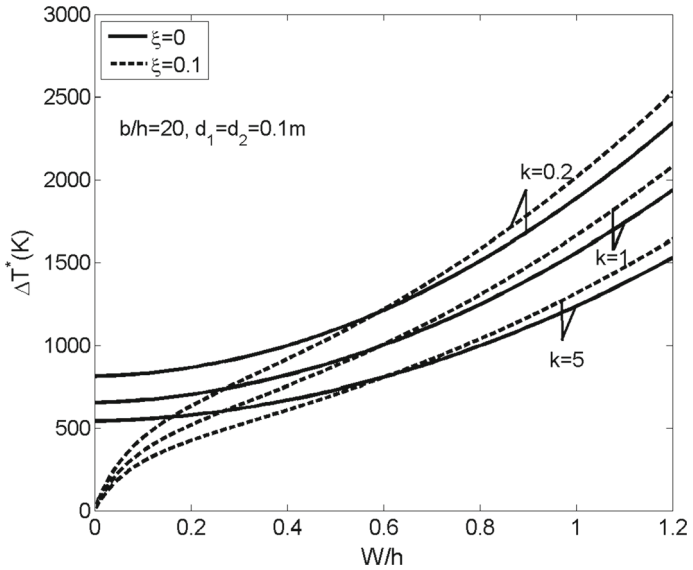

Fig. 4 Effect of the volume fraction index k on the postbuckling behavior of ES-FGM plates under nonlinear temperature change

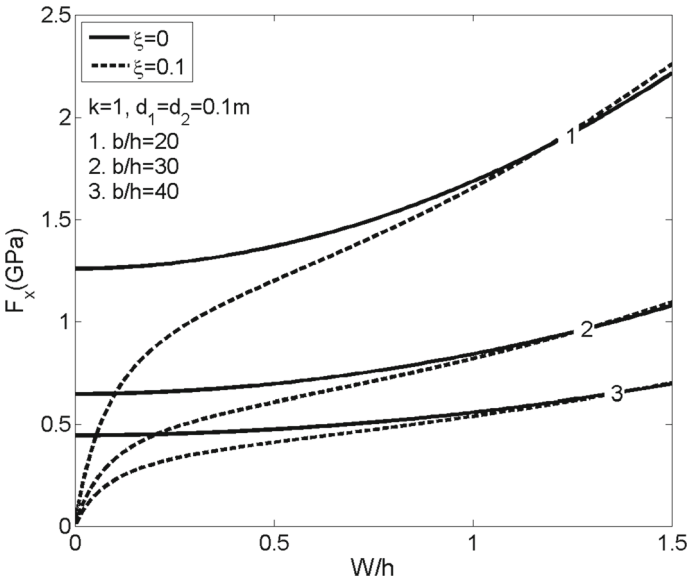

Fig. 5 Effect of side-to-thickness ratio b/h on the postbuckling behavior of an ES-FGM on elastic foundations under uniaxial compression

Figure 4 illustrates the effect of volume fraction index k on postbuckling $\Delta T - W/h$ curves of ES-FGM plates on an elastic foundation with the nonlinear change of temperature.

From these Figures, it can be seen that the postbuckling curves become higher when the value of k decreases. This property is appropriate to the real characteristic of the material, because the smaller value of k corresponds to the richer ceramic, and the plate has the better load-carrying capacity (Fig. 3) or the plate becomes better thermal barrier structure (Fig. 4).

8.2.2 Effect of geometric parameters

Figure 5 shows the effect of the ratio b/h on postbuckling $F_x - W/h$ curves of an ES-FGM plate on elastic foundations under uniaxial compression. It can be observed that the postbuckling load–deflection curves become lower when the values of b/h increase.

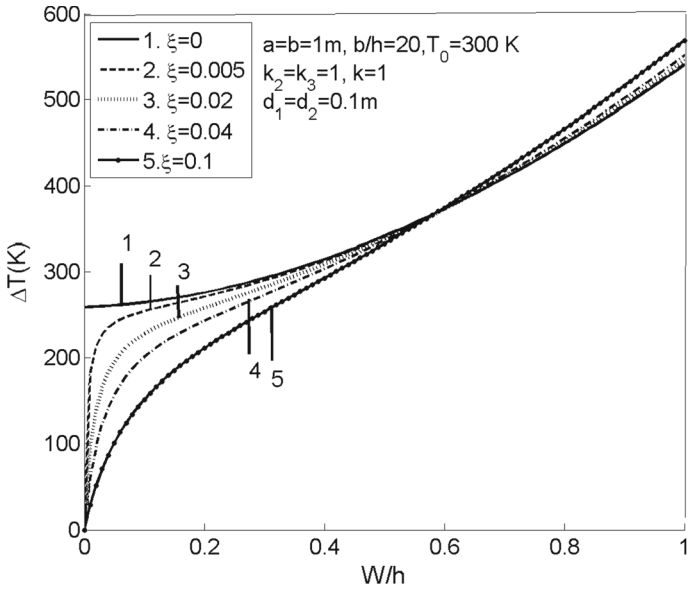

Fig. 6 Effect of imperfection on the thermal nonlinear response of immovable edge ES-FGM plates (T-D)

Table 5 Critical compressive load F_x^{cr} (GPa) for different number of stiffeners and material of stiffener of ES-FGM plates ($\eta = 1, k = 1$)

The number of stiffeners	F_x^{cr}(GPa)	
	$a/b = 1$	$a/b = 1.5$
Without stiffeners	1.2014	0.9048
5+5 Orthogonal stiffeners	1.2298	0.9270
10+10 Orthogonal stiffeners	1.2580	0.9489
20+20 Orthogonal stiffeners	1.3137	0.9917
40+40 Orthogonal stiffeners	1.4220	1.0740

Table 6 The critical thermal load ΔT_{cr} (K) for ES-FGM plates subjected to uniform temperature rise with temperature-dependent properties (T-D properties)

a/b	k	Arrangement of stiffeners			
		Without stiffeners	20 Longitudinal stiffeners	20 Transversal stiffeners	Orthogonal stiffeners (10+10)
0.75	0.2	395.38[a] (504.22[b])	415.73 (536.55)	402.27 (515.13)	409.52 (526.63)
	1	326.17 (397.34)	341.67 (420.17)	331.23 (404.78)	336.85 (413.05)
	5	289.05 (342.19)	302.75 (361.17)	293.47 (348.30)	298.47 (355.22)
1	0.2	306.75 (371.66)	315.86 (384.80)	315.86 (384.80)	316.17 (385.25)
	1	251.63 (293.63)	258.40 (302.78)	258.40 (302.78)	258.64 (303.11)
	5	221.95 (253.49)	227.81 (261.06)	227.81 (261.06)	228.02 (261.33)
1.5	0.2	239.56 (278.66)	241.57 (281.36)	249.56 (292.09)	245.73 (286.92)
	1	195.99 (221.15)	197.38 (222.92)	203.45 (230.61)	200.54 (226.92)
	5	172.61 (191.65)	173.77 (193.07)	179.02 (199.50)	176.50 (196.41)

[a] T-D, [b] T-ID

Table 6 gives the effect of the ratio a/b on the critical thermal load ΔT_{cr} (K) for ES-FGM plates subjected to the uniform temperature rise with temperature-dependent properties. As can be seen, the values of the critical thermal loads with $a/b = 0.75$ are largest, but the ones with $a/b = 1$ are smaller, and the ones with $a/b = 1.5$ are smallest.

Figure 6 shows effects of imperfection on the nonlinear response of plates exposed to the uniform temperature field with temperature-dependent properties. It is observed that the postbuckling load-carrying capacity of plates is reduced with the increase in imperfection size ξ when the deflection is still small, but an inverse trend occurs when the deflection is sufficiently large.

8.2.3 Effect of stiffeners

Table 5 shows effects of the stiffener number on the critical mechanical load. It can be seen that the critical load increases with the increased number of stiffeners. This increase is considerable. For example, $F_x^{\mathrm{cr}} = 1.422\,\mathrm{GPa}$ (40+40 orthogonal stiffeners) increases about 7.6 % in comparison with $F_x^{\mathrm{cr}} = 1.3137\,\mathrm{GPa}$ (20+20 orthogonal stiffeners).

Table 6 presents the effects of different stiffener types as longitudinal stiffeners, transversal stiffeners and orthogonal stiffeners on critical buckling loads of the FGM plate. It can be seen that these types of stiffeners affect strongly the critical thermal load of the plate.

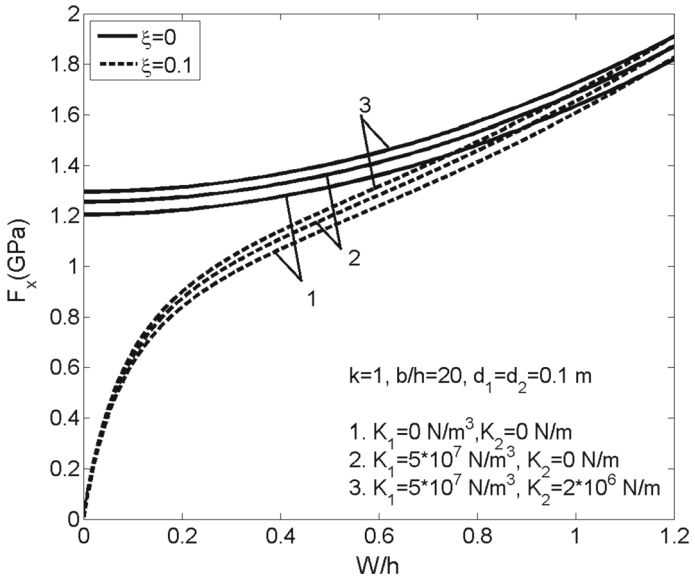

Fig. 7 Effect of foundations on the postbuckling behavior of ES-FGM on elastic foundations under uniaxial compression

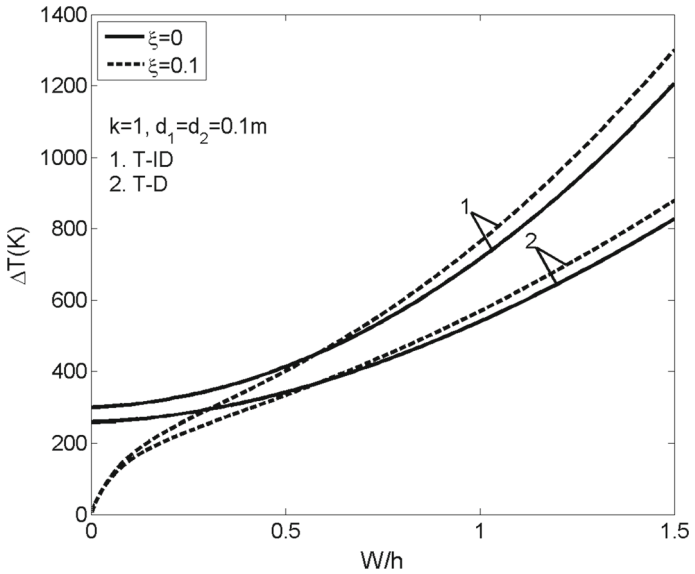

Fig. 8 Thermal postbuckling of ES-FGM plates on a foundation with temperature-independent (T-ID) and temperature-dependent (T-D) properties

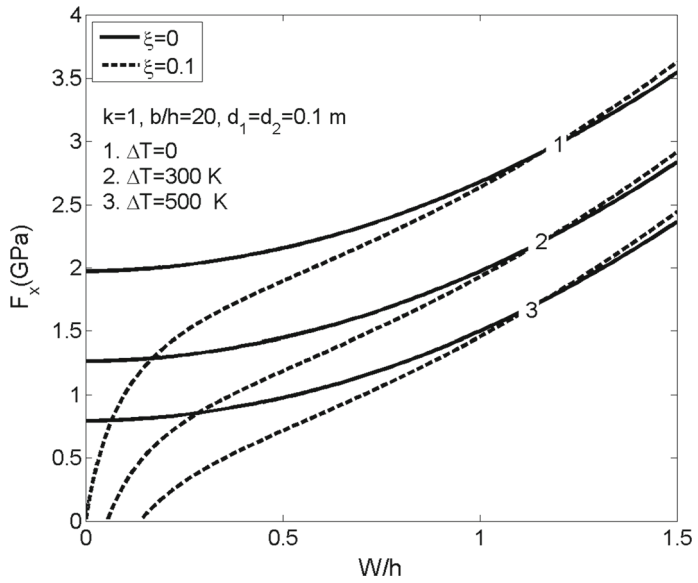

Fig. 9 Effect of increasing temperature field on the postbuckling behavior of ES-FGM plates under uniaxial compression

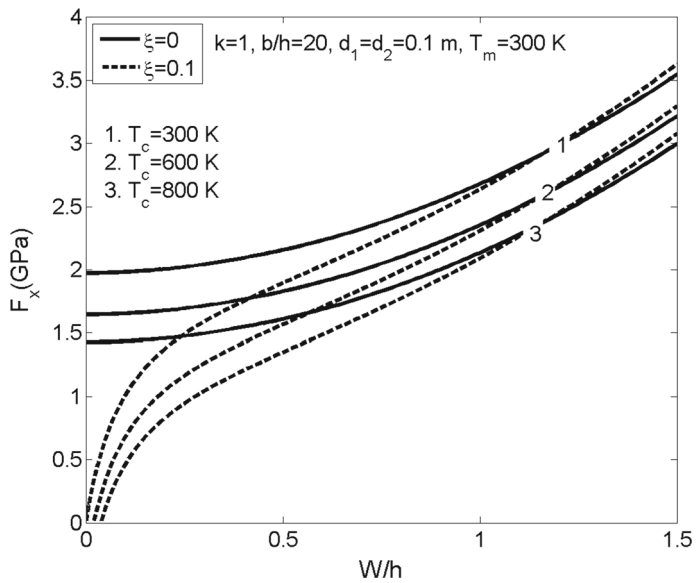

Fig. 10 Effect of nonlinear temperature change on the postbuckling behavior of ES-FGM plates under uniaxial compression

8.2.4 Effect of elastic foundations

Figure 7 shows effects of elastic foundations on postbuckling $F_x - W/h$ curves and $\Delta T - W/h$ of an ES-FGM plate by using Eq. (36). As can be observed, the curve corresponding to both parameters of foundation $K_1 \neq 0$, $K_2 \neq 0$ is the highest, the one corresponding to without foundation is the lowest.

8.2.5 Effect of temperature on postbuckling load–deflection curves of orthogonally stiffened FGM plates

Figure 8 shows the effect of temperature on postbuckling $\Delta T - W/h$ curves of an ES-FGM plate ($a = b$) for two cases T-ID and T-D material properties. It is evident that the postbuckling load-carrying capacity of the plate is strongly reduced.

Figures 9 and 10 show the effects of temperature on postbuckling $F_x - W/h$ curves of ES-FGM square plates under mechanical compression load on elastic foundations for T-ID with uniform temperature rise and

Table 7 The value of critical thermal loads ΔT_{cr} (K) in two cases of an FGM plate: uniform temperature rise and nonlinear temperature change

	k	Uniform temperature rise		Nonlinear temperature change	
		$K_1 = 0$, K_2=0	$K_1 = 5\times10^7$ N/m^3, $K_2 = 10^5$ N/m	$K_1 = 0$, K_2=0	$K_1 = 5\times10^7$ N/m^3, $K_2 = 10^5$ N/m
Without stiffeners	0.2	357.49	371.83	753.71	783.95
	0.5	312.23	325.69	673.04	702.06
	1	280.83	293.70	606.89	634.71
	5	241.38	253.52	502.25	527.52
Orthogonal FGM stiffeners	0.2	371.29	385.43	783.04	812.87
	0.5	323.59	336.87	697.69	726.32
	1	290.49	303.19	627.77	655.20
	5	249.39	261.36	518.78	543.68

nonlinear temperature change. It can be seen that the postbuckling curves become lower gradually with the increase in temperature. This is reasonable because the preheated ES-FGM plates exhibit a decreasing tendency in the postbuckling load- carrying capacity when they are subjected to added action of mechanical loads.

Table 7 shows values of critical thermal loads ΔT_{cr} (K) for two cases of uniform temperature rise and nonlinear temperature change. As can be seen, the critical thermal loads of FGM plates under uniform temperature rise are smaller than those under nonlinear temperature change.

9 Conclusions

This paper presents buckling and postbuckling nonlinear analyses of imperfect FGM plates reinforced by FGM stiffeners on elastic foundations and subjected to in-plane compressive mechanical loads or thermal loads or thermo-mechanical loads simultaneously by an analytical approach. The material properties of plate and stiffeners are assumed to be T-D or T-ID and graded in the thickness direction according to a volume fraction power-law distribution. Based on the Reddy's TSDT with the von Kármán kinematic nonlinearity and taking into account stiffener, four nonlinear stability equations for ES-FGM plates are derived. Equations (10–13.1) are the most important relations found in this work in which the contribution of stiffeners and thermal elements in equations of N_{ij}, M_{ij}, P_{ij}, Q_i, R_i are taken into account. The closed-form expressions for determining the buckling load and analyzing postbuckling load–deflection curves are obtained by the Galerkin method. Two iterative algorithms are presented for the case of temperature-dependent plate material properties. The effects of temperature, stiffener, material properties, geometrical parameters, and foundation parameters are analyzed in detail by numerical calculations. The comparisons show that the present results are in good agreement with the existing previous results and therefore affirmed the reliability and accuracy of the proposed method. Some remarks are deduced from the present results as:

(i) Reddy's third-order shear deformation theory can represent better the kinematic behavior and may not require shear correction factors. This is also the main reason why this theory is used to investigate the nonlinear buckling and postbuckling of thicker FGM plates.
(ii) The postbuckling mechanical load–deflection curves lower gradually with increase of ΔT.
(iii) The presence of stiffeners enhances the stability of FGM plates.
(iv) The thermal element, stiffener, foundation parameters and volume index affect strongly buckling and postbuckling behavior of plates.

Appendix I

$$E_i = \int_{-h/2}^{h/2} z^{i-1} E_{\mathrm{p}}(z, T)\,\mathrm{d}z, \quad i = 1, 2, 3, 4, 5, 7,$$

$$E_i^{sx} = \int_{h/2}^{h_1+h/2} z^{i-1} E_{sx}(z)\,dz, \quad E_i^{sy} = \int_{h/2}^{h_2+h/2} z^{i-1} E_{sy}(z)\,dz, \quad i = 1,2,3,4,5,7,$$

$$a_{11} = \left(\frac{E_1}{1-\nu^2} + \frac{b_1 E_1^{sx}}{d_1}\right), \quad a_{12} = \frac{E_1\nu}{1-\nu^2}, \quad a_{13} = \frac{E_2}{1-\nu^2} + \frac{b_1 E_2^{sx}}{d_1} - \lambda\left(\frac{E_4}{1-\nu^2} + \frac{b_1 E_4^{sx}}{d_1}\right),$$

$$a_{14} = \frac{E_2\nu}{1-\nu^2} - \lambda\frac{E_4\nu}{1-\nu^2}, \quad a_{15} = -\lambda\left(\frac{E_4}{1-\nu^2} + \frac{b_1 E_4^{sx}}{d_1}\right), \quad a_{16} = -\lambda\frac{E_4\nu}{1-\nu^2},$$

$$a_{17} = -\frac{1}{1-\nu}, \quad a_{18} = -\frac{b_1}{d_1},$$

$$a_{21} = \frac{E_1\nu}{1-\nu^2} = a_{12}, \quad a_{22} = \frac{E_1}{1-\nu^2} + \frac{b_2 E_1^{sy}}{d_2}, \quad a_{23} = \frac{E_2\nu}{1-\nu^2} - \lambda\frac{E_4\nu}{1-\nu^2},$$

$$a_{24} = \frac{E_2}{1-\nu^2} + \frac{b_2 E_2^{sy}}{d_2} - \lambda\left(\frac{E_4}{1-\nu^2} + \frac{b_2 E_4^{sy}}{d_2}\right), \quad a_{25} = -\lambda\frac{E_4\nu}{1-\nu^2} = a_{16},$$

$$a_{26} = -\lambda\left(\frac{E_4}{1-\nu^2} + \frac{b_2 E_4^{sy}}{d_2}\right), \quad a_{27} = -\frac{1}{1-\nu} = a_{17}, \quad a_{28} = -\frac{b_2}{d_2},$$

$$a_{31} = \frac{E_1}{2(1+\nu)}, \quad a_{32} = \frac{E_2}{2(1+\nu)} - \lambda\frac{E_4}{2(1+\nu)}, \quad a_{33} = a_{32}, \quad a_{34} = -\lambda\frac{E_4}{1+\nu},$$

$$b_{11} = \frac{E_2}{1-\nu^2} + \frac{b_1 E_2^{sx}}{d_1}, \quad b_{12} = \frac{E_2\nu}{1-\nu^2},$$

$$b_{13} = \frac{E_3}{1-\nu^2} + \frac{b_1 E_3^{sx}}{d_1} - \lambda\left(\frac{E_5}{1-\nu^2} + \frac{b_1 E_5^{sx}}{d_1}\right), \quad b_{14} = \frac{E_3\nu}{1-\nu^2} - \lambda\frac{E_5\nu}{1-\nu^2},$$

$$b_{15} = -\lambda\left(\frac{E_5}{1-\nu^2} + \frac{b_1 E_5^{sx}}{d_1}\right), \quad b_{16} = -\lambda\frac{E_5\nu}{1-\nu^2},$$

$$b_{17} = -\frac{1}{1-\nu} = a_{17}, \quad b_{18} = -\frac{b_1}{d_1} = a_{18},$$

$$b_{21} = \frac{E_2\nu}{1-\nu^2} = b_{12}, \quad b_{22} = \frac{E_2}{1-\nu^2} + \frac{b_2 E_2^{sy}}{d_2}, \quad b_{23} = \frac{E_3\nu}{1-\nu^2} - \lambda\frac{E_5\nu}{1-\nu^2},$$

$$b_{24} = \frac{E_3}{1-\nu^2} + \frac{b_2 E_3^{sy}}{d_2} - \lambda\left(\frac{E_5}{1-\nu^2} + \frac{b_2 E_5^{sy}}{d_2}\right), \quad b_{25} = -\lambda\frac{E_5\nu}{1-\nu^2} = b_{16},$$

$$b_{26} = -\lambda\left(\frac{E_5}{1-\nu^2} + \frac{b_2 E_5^{sy}}{d_2}\right), \quad b_{27} = -\frac{1}{1-\nu} = b_{17}, \quad b_{28} = -\frac{b_2}{d_2},$$

$$b_{31} = \frac{E_2}{2(1+\nu)}, \quad b_{32} = \frac{E_3}{2(1+\nu)} - \lambda\frac{E_5}{2(1+\nu)}, \quad b_{33} = b_{32}, \quad b_{34} = -\lambda\frac{E_5}{1+\nu},$$

$$c_{11} = \frac{E_4}{1-\nu^2} + \frac{b_1 E_4^{sx}}{d_1}, \quad c_{12} = \frac{E_4\nu}{1-\nu^2}, \quad c_{13} = \frac{E_5}{1-\nu^2} + \frac{b_1 E_5^{sx}}{d_1} - \lambda\left(\frac{E_7}{1-\nu^2} + \frac{b_1 E_7^{sx}}{d_1}\right),$$

$$c_{14} = \frac{E_5\nu}{1-\nu^2} - \lambda\frac{E_7\nu}{1-\nu^2}, \quad c_{15} = -\lambda\left(\frac{E_7}{1-\nu^2} + \frac{b_1 E_7^{sx}}{d_1}\right), \quad c_{16} = -\lambda\frac{E_7\nu}{1-\nu^2},$$

$$c_{17} = -\frac{1}{1-\nu} = a_{17}, \quad c_{18} = -\frac{b_1}{d_1},$$

$$c_{21} = \frac{E_4\nu}{1-\nu^2} = c_{12}, \quad c_{22} = \frac{E_4}{1-\nu^2} + \frac{b_2 E_4^{sy}}{d_2}, \quad c_{23} = \frac{E_5\nu}{1-\nu^2} - \lambda\frac{E_7\nu}{1-\nu^2},$$

$$c_{24} = \frac{E_5}{1-\nu^2} + \frac{b_2 E_5^{sy}}{d_2} - \lambda\left(\frac{E_7}{1-\nu^2} + \frac{b_2 E_7^{sy}}{d_2}\right), \quad c_{25} = -\lambda\frac{E_7\nu}{1-\nu^2} = b_{16},$$

$$c_{26}=-\lambda\left(\frac{E_7}{1-\nu^2}+\frac{b_2E_7^{sy}}{d_2}\right),\quad c_{27}=-\frac{1}{1-\nu}=a_{17},\quad c_{28}=-\frac{b_2}{d_2},$$
$$c_{31}=\frac{E_4}{2\left(1+\nu\right)},\quad c_{32}=\frac{E_5}{2\left(1+\nu\right)}-\lambda\frac{E_7}{2\left(1+\nu\right)},\quad c_{33}=c_{32},\quad c_{34}=-\lambda\frac{E_7}{1+\nu},$$
$$d_{11}=\frac{E_1}{2\left(1+\nu\right)}+\frac{b_1}{d_1}\frac{E_1^{sx}}{2\left(1+\nu\right)}-3\lambda\left[\frac{E_3}{2\left(1+\nu\right)}+\frac{b_1}{d_1}\frac{E_3^{sx}}{2\left(1+\nu\right)}\right],\quad d_{12}=d_{11},$$
$$d_{21}=\frac{E_1}{2\left(1+\nu\right)}+\frac{b_2}{d_2}\frac{E_1^{sy}}{2\left(1+\nu\right)}-3\lambda\left[\frac{E_3}{2\left(1+\nu\right)}+\frac{b_2}{d_2}\frac{E_3^{sy}}{2\left(1+\nu\right)}\right],\quad d_{22}=d_{21},$$
$$e_{11}=\frac{E_3}{2\left(1+\nu\right)}+\frac{b_1}{d_1}\frac{E_3^{sx}}{2\left(1+\nu\right)}-3\lambda\left[\frac{E_5}{2\left(1+\nu\right)}+\frac{b_1}{d_1}\frac{E_5^{sx}}{2\left(1+\nu\right)}\right],\quad e_{12}=e_{11},$$
$$e_{21}=\frac{E_3}{2\left(1+\nu\right)}+\frac{b_2}{d_2}\frac{E_3^{sy}}{2\left(1+\nu\right)}-3\lambda\left[\frac{E_5}{2\left(1+\nu\right)}+\frac{b_2}{d_2}\frac{E_5^{sy}}{2\left(1+\nu\right)}\right],\quad e_{22}=e_{21}.$$

Appendix II

$$\delta_m=\frac{1-(-1)^m}{2},\quad \delta_n=\frac{1-(-1)^n}{2},\quad G_3=-\frac{a_{23}^*\alpha^3+\left(a_{13}^*-a_{32}^*\right)\alpha\beta^2}{a_{22}^*\alpha^4+\left(a_{12}^*+a_{21}^*+a_{31}^*\right)\alpha^2\beta^2+a_{11}^*\beta^4},$$
$$G_4=-\frac{\left(a_{24}^*-a_{33}^*\right)\alpha^2\beta+a_{14}^*\beta^3}{a_{22}^*\alpha^4+\left(a_{12}^*+a_{21}^*+a_{31}^*\right)\alpha^2\beta^2+a_{11}^*\beta^4},\quad G_5=-\frac{a_{25}^*\alpha^4+\left(a_{15}^*+a_{26}^*-a_{34}^*\right)\alpha^2\beta^2+a_{16}^*\beta^4}{a_{22}^*\alpha^4+\left(a_{12}^*+a_{21}^*+a_{31}^*\right)\alpha^2\beta^2+a_{11}^*\beta^4},$$
$$l_{11}=b_{15}^*\alpha^4+\left(b_{16}^*+b_{25}^*+2b_{34}^*\right)\alpha^2\beta^2+b_{26}^*\beta^4-K_1-K_2\left(\alpha^2+\beta^2\right)$$
$$+G_5\left[b_{12}^*\alpha^4+\left(b_{11}^*+b_{22}^*-2b_{31}^*\right)\alpha^2\beta^2+b_{21}^*\beta^4\right],$$
$$l_{12}=b_{13}^*\alpha^3+\left(b_{23}^*+2b_{32}^*\right)\alpha\beta^2+G_3\left[b_{12}^*\alpha^4+\left(b_{11}^*+b_{22}^*-2b_{31}^*\right)\alpha^2\beta^2+b_{21}^*\beta^4\right],$$
$$l_{13}=\left(b_{14}^*+2b_{33}^*\right)\alpha^2\beta+b_{24}^*\beta^3+G_4\left[b_{12}^*\alpha^4+\left(b_{11}^*+b_{22}^*-2b_{31}^*\right)\alpha^2\beta^2+b_{21}^*\beta^4\right],$$
$$l_{14}=G_3\frac{32\alpha^2\beta^2}{3mn\pi^2}\delta_m\delta_n,\quad l_{15}=G_4\frac{32\alpha^2\beta^2}{3mn\pi^2}\delta_m\delta_n,$$
$$l_{21}=\left(b_{15}^*-\lambda c_{15}^*\right)\alpha^3+\left[\left(b_{16}^*+b_{34}^*\right)-\lambda\left(c_{16}^*+c_{34}^*\right)\right]\alpha\beta^2+\left(d_{12}-3\lambda e_{12}\right)\alpha$$
$$+\left\{\left(b_{12}^*-\lambda c_{12}^*\right)\alpha^3+\left[\left(b_{11}^*-b_{31}^*\right)-\lambda\left(c_{11}^*-c_{31}^*\right)\right]\alpha\beta^2\right\}G_5,$$
$$l_{22}=\left(b_{13}^*-\lambda c_{13}^*\right)\alpha^2+\left(b_{32}^*-\lambda c_{32}^*\right)\beta^2+\left(d_{11}-3\lambda e_{11}\right)+\left\{\left(b_{12}^*-\lambda c_{12}^*\right)\alpha^3\right.$$
$$\left.+\left[\left(b_{11}^*-b_{31}^*\right)-\lambda\left(c_{11}^*-c_{31}^*\right)\right]\alpha\beta^2\right\}G_3,$$
$$l_{23}=\left[\left(b_{14}^*+b_{33}^*\right)-\lambda\left(c_{14}^*+c_{33}^*\right)\right]\alpha\beta+\left\{\left(b_{12}^*-\lambda c_{12}^*\right)\alpha^3+\left[\left(b_{11}^*-b_{31}^*\right)-\lambda\left(c_{11}^*-c_{31}^*\right)\right]\alpha\beta^2\right\}G_4,$$
$$l_{31}=\left(b_{26}^*-\lambda c_{26}^*\right)\beta^3+\left[\left(b_{25}^*+b_{34}^*\right)-\lambda\left(c_{25}^*+c_{34}^*\right)\right]\alpha^2\beta$$
$$+\left(d_{22}-3\lambda e_{22}\right)\beta+\left\{\left(b_{21}^*-\lambda c_{21}^*\right)\beta^3+\left[\left(b_{22}^*-b_{31}^*\right)-\lambda\left(c_{22}^*-c_{31}^*\right)\right]\alpha^2\beta\right\}G_5,$$
$$l_{32}=\left[\left(b_{23}^*+b_{32}^*\right)-\lambda\left(c_{23}^*+c_{32}^*\right)\right]\alpha\beta+\left\{\left(b_{21}^*-\lambda c_{21}^*\right)\beta^3+\left[\left(b_{22}^*-b_{31}^*\right)-\lambda\left(c_{22}^*-c_{31}^*\right)\right]\alpha^2\beta\right\}G_3,$$
$$l_{33}=\left(b_{33}^*-\lambda c_{33}^*\right)\alpha^2+\left(b_{24}^*-\lambda c_{24}^*\right)\beta^2+d_{21}-3\lambda e_{21}+\left\{\left(b_{21}^*-\lambda c_{21}^*\right)\beta^3\right.$$
$$\left.+\left[\left(b_{22}^*-b_{31}^*\right)-\lambda\left(c_{22}^*-c_{31}^*\right)\right]\alpha^2\beta\right\}G_4,$$
$$s_1=G_5\frac{32\alpha^2\beta^2}{3mn\pi^2}\delta_m\delta_n s_2=\frac{-8\alpha^2\beta^2}{3mn\pi^2}\left(\frac{b_{12}^*}{a_{22}^*}+\frac{b_{21}^*}{a_{11}^*}\right)\delta_m\delta_n,\quad s_3=\frac{-1}{16}\left(\frac{\beta^4}{a_{22}^*}+\frac{\alpha^4}{a_{11}^*}\right),\quad s_4=\frac{16}{mn\pi^2}\delta_m\delta_n,$$
$$s_5=\frac{-8\alpha\beta^2}{3mn\pi^2}\left(\frac{b_{12}^*-\lambda c_{12}^*}{a_{22}^*}\right)\delta_m\delta_n,\quad s_6=\frac{-8\alpha^2\beta}{3mn\pi^2}\left(\frac{b_{21}^*-\lambda c_{21}^*}{a_{11}^*}\right)\delta_m\delta_n.$$

References

1. Ferreira, A.J.M., Roque, C.M.C., Neves, A.M.A., Jorge, R.M.N., Soares, C.M.M., Reddy, J.N.: Buckling analysis of isotropic and laminated plates by radial basis functions according to a higher-order shear deformation theory. Thin Walled Struct. **49**, 804–811 (2011)
2. Samsam Shariat, B.A., Eslami, M.R.: Buckling of thick functionally graded plates under mechanical and thermal loads. Compos. Struct. **78**, 433–439 (2007)
3. Khabbaz, R.S., Manshadi, B.D., Abedian, A.: Nonlinear analysis of FGM plates under pressure loads using the higher-order shear deformation theories. Compos. Struct. **89**, 333–344 (2009)
4. Duc, N.D., Tung, H.V.: Mechanical and thermal postbuckling of higher order shear deformable functionally graded plates on elastic foundations. Compos. Struct. **93**, 2874–2881 (2011)
5. Javaheri, R., Eslami, M.R.: Buckling of functionally graded plates under in-plane compressive loading. J. Appl. Math. Mech. **82**, 277–283 (2002)
6. Javaheri, R., Eslami, M.R.: Thermal buckling of functionally graded plates. AIAA J. **40**, 162–169 (2002)
7. Javaheri, R., Eslami, M.R.: Thermal buckling of functionally graded plates based on the higher order theory. J. Therm. Stress **25**, 603–25 (2002)
8. Na, K.S., Kim, J.H.: Three-dimensional thermo–mechanical buckling analysis for functionally graded composite plates. Compos. Struct. **73**, 413–422 (2006)
9. Lanhe, W.: Thermal buckling of a simply supported moderately thick rectangular FGM plate. Compos. Struct. **64**, 211–218 (2004)
10. Kiani, Y., Eslami, M.R.: An exact solution for thermal buckling of annular FGM plates on an elastic medium. Compos. B Eng. **45**, 101–110 (2013)
11. Hui, D., Du, I.H.Y.: Initial postbuckling behavior of imperfect antisymmetric crossply cylindrical shells under torsion. J. Appl. Mech. ASME **54**, 174–180 (1987)
12. Zhang, X., Han, Q.: Buckling and postbuckling behaviors of imperfect cylindrical shells subjected to torsion. Thin Wall. Struct. **45**, 1035–1043 (2007)
13. Jiang, Q., Wang, X., Zhu, Y., Hui, D., Qiu, Y.: Mechanical, electrical and thermal properties of aligned carbon nanotube/polyimide composites. Compos. B Eng. **56**, 408–412 (2014)
14. Bagherizadeh, E., Kiani, Y., Eslami, M.R.: Mechanical buckling of functionally graded material cylindrical shells surrounded by Pasternak elastic foundation. Compos. Struct. **93**, 3063–3071 (2011)
15. Najafov, A.M., Sofiyev, A.H., Kuruoglu, N.: Torsional vibration and stability of functionally graded orthotropic cylindrical shells on elastic foundations. Meccanica **48**, 829–840 (2013)
16. Sofiyev, A.H., Avcar, M.: The stability of cylindrical shells containing a FGM layer subjected to axial load on the Pasternak foundation. Engineering **2**, 228–236 (2010)
17. Sofiyev, A.H., Kuruoglu, N.: Torsional vibration and buckling of the cylindrical shell with functionally graded coatings surrounded by an elastic medium. Compos. B Eng. **45**, 1133–1142 (2013)
18. Sofiyev, A.H.: The buckling of FGM truncated conical shells subjected to axial compressive load and resting on Winkler-Pasternak foundations. Int. J. Press. Vessels Pip. **87**, 753–761 (2010)
19. Sofiyev, A.H.: Non-linear buckling behavior of FGM truncated conical shells subjected to axial load. Int. J. Nonlinear Mech. **46**, 711–719 (2011)
20. Sofiyev, A.H.: Non-linear buckling of an FGM truncated conical shell surrounded by an elastic medium. Int. J. Press. Vessels Pip. **107**, 38–49 (2013)
21. Shen, H.S.: Thermal postbuckling behavior of functionally graded cylindrical shells with temperature-dependent properties. Int. J. Solids Struct. **41**, 1961–1974 (2004)
22. Shen, H.S.: Thermal postbuckling behavior of shear deformable FGM plates with temperature-dependent properties. Int. J. Mech. Sci. **49**, 466–478 (2007)
23. Shen, H.S., Wang, Z.X.: Nonlinear bending of FGM plates subjected to combined loading and resting on elastic foundations. Compos. Struct. **92**, 2517–2524 (2010)
24. Lal, A., Jagtap, K.R., Singh, B.N.: Postbuckling response of functionally graded materials plate subjected to mechanical and thermal loadings with random material properties. Appl. Math. Model. **37**, 2900–2920 (2013)
25. Akbari, M., Kiani, Y., Eslami, M.R.: Thermal buckling of temperature-dependent FGM conical shells with arbitrary edge supports. Acta Mech. **226**, 897–915 (2015)
26. Mirzavand, B., Eslami, M.R.: A closed-form solution for thermal buckling of piezoelectric FGM rectangular plates with temperature-dependent properties. Acta Mech. **218**, 87–101 (2011)
27. Timoshenko, S.P., Gere, J.M.: Theory of Elastic Stability. McGraw-Hill, New York (1961)
28. Steen, E.: Elastic buckling and postbuckling of eccentrically stiffened plates. Int. J. Solids Struct. **25**, 751–768 (1989)
29. Bedair, O.K.: Influence of stiffener location on the stability of stiffened plates under compression and in-plane bending. Int. J. Mech. Sci. **39**, 33–49 (1997)
30. Bich, D.H., Dung, D.V., Nam, V.H.: Nonlinear dynamical analysis of eccentrically stiffened functionally graded cylindrical panels. Compos. Struct. **94**, 2465–2473 (2012)
31. Najafizadeh, M.M., Hasani, A., Khazaeinejad, P.: Mechanical stability of functionally graded stiffened cylindrical shells. Appl. Math. Model. **33**, 1151–1157 (2009)
32. Dung, D.V., Nam, V.H.: Nonlinear dynamic analysis of eccentrically stiffened functionally graded circular cylindrical thin shells under external pressure and surrounded by an elastic medium. Eur. J. Mech. A/Solids **46**, 42–53 (2014)
33. Dung, D.V., Hoa, L.K., Nga, N.T.: On the stability of functionally graded truncated conical shells reinforced by functionally graded stiffeners and surrounded by an elastic medium. Compos. Struct. **108**, 77–90 (2014)
34. Dung, D.V., Hoa, L.K.: Nonlinear torsional buckling and postbuckling of eccentrically stiffened FGM cylindrical shells in thermal environment. Compos. B Eng. **69**, 378–388 (2015)
35. Reddy, J.N.: A simple higher-order theory for laminated composite plates. J. Appl. Mech. **51**, 745–752 (1984)

36. Reddy, J.N.: Analysis of functionally graded plates. Int. J. Numer. Methods Eng. **47**, 663–684 (2000)
37. Reddy, J.N.: Mechanics of Laminated Composite Plates and Shells: Theory and Analysis. CRC Press LLC, Boca Raton (2004)
38. Shen, H.S.: Functionally Graded Materials; Nonlinear Analysis of Plates and Shells. CRC Press LLC, Boca Raton (2009)
39. Brush, D.O., Almroth, B.O.: Buckling of Bars, Plates and Shells. McGraw-Hill, New York (1975)
40. Birman, V., Bert, C.W.: Dynamic stability of reinforced composite cylindrical shells in thermal fields. J. Sound Vib. **142**, 183–190 (1990)
41. Thai, H.-T., Choi, D.-H.: Analytical solutions of refined plate theory for bending buckling and vibration analyses of thick plates. Appl. Math. Model. **37**, 8310–8323 (2013)
42. Reddy, J.N., Chin, C.D.: Thermo–mechanical analysis of functionally graded cylinders and plates. J. Therm. Stress **21**, 593–626 (1998)